A UNITED STATES DEPARTMENT OF COMMERCE PUBLICATION

BOMEX

Period III Radar-Satellite Atlas

U. S. DEPARTMENT OF COMMERCE

National Oceanic and Atmospheric Administration

Environmental Data Service

U.S. DEPARTMENT OF COMMERCE
National Oceanic and Atmospheric Administration
Environmental Data Service

BOMEX

Period III Radar-Satellite Atlas

Wolfgang D. Scherer
Michael D. Hudlow

Center for Experiment Design and Data Analysis

Washington, D.C.
January 1975

The National Oceanic and Atmospheric Administration does not approve, recommend, or endorse any product except for its own use, and naming of a product or a manufacturer is solely for purposes of identification. The evaluation and test results shall not be used in advertising, sales promotion, or to indicate in any manner, either implicitly or explicitly, endorsement by the National Oceanic and Atmospheric Administration.

ACKNOWLEDGMENTS

The authors are indebted to Briah Connor for his assistance in selecting and mosaicing the radar pictures, to Vance Myers and Martin Predoehl for their assistance in obtaining and validating the gridding accuracy of the ATS-III data, to Norbert Delver who was responsible for renavigating ship positions, to May Laughrun for her editorial assistance, and to Pat McNair for typing the manuscript.

INTRODUCTION

Clouds and their precipitation are of importance in many studies of the atmosphere. For this reason, the atmosphere was sampled by both satellites and radars during the Barbados Oceanographic and Meteorological Experiment (BOMEX), conducted in 1969. A principal objective of BOMEX was to measure the rate of exchange of the "properties" of heat, water substance, and momentum between the tropical ocean and the atmosphere. As an experimental prototype of the basic grid element of a global observation system, an area 500 km by 500 km east of Barbados was chosen for the field operations. Meteorological and oceanographic data were gathered by ships, aircraft, and buoys, supplemented by satellite data and by land-based observations on the island of Barbados.

The field operations were divided into four observation periods of 13 to 18 days each to support the two major investigations: the air-sea interaction investigation, conducted during BOMEX Period I, May 3 to May 15, Period II, May 24 to June 10, and Period III, June 19 to July 2, 1969; and the investigation of tropical convective systems, conducted during Period IV, July 11 to July 28, 1969.

Two surface-based radars, one located on the island of Barbados and the other on the NOAA ship *Discoverer,* provided radar coverage only over the southern half of the BOMEX array shown in figure 1. This spatial limitation in surface-based radar coverage suggested the use of information provided by satellites in order to derive precipitation estimates for the entire BOMEX area. Additional data were obtained by a radar carried aboard U.S. Air Force Air Weather Service WB-47 aircraft.

The products included in this atlas fall into two categories: (1) composites of data from the two surface-based radars and from the airborne radar on the WB-47 aircraft, and (2) satellite photographs and maps consisting of Applied Technology Satellite III (ATS III) cloud photographs and Nimbus 3 high-resolution infrared radiometer (HRIR) and medium-resolution infrared radiometer (MRIR) minimum cloud top maps.

The selection of these products is based on one major determining factor: a close time match between the radar composites and the satellite products. This criterion fixes two of the four times: nominally 0330 GMT, when both HRIR and MRIR data are available, and nominally 1500 GMT, when MRIR and ATS III information was obtained. The other two times at nominally 1100 and 2000 GMT were selected corresponding to early morning and late afternoon, when there was good sunlight illumination over the BOMEX area.

Of overriding importance for meaningful intercomparison of the various data products was to reproduce the data covering the BOMEX square in all cases at the same scale. For the surface-based radar composites this required some fairly involved procedures, which are discussed later.

This atlas covers BOMEX Period III only. The date and time of each of the displays is given in table 1. Surface-based and airborne radar data for the other three periods are available from the BOMEX Permanent Archive, National Climatic Center, National Oceanic and Atmospheric Administration, Federal Building, Asheville, N.C. 28801.

SURFACE RADAR COMPOSITES

The radar photographs used for the surface radar composites were collected by two X-band (3 cm) radars.

The U.S. Army Atmospheric Sciences Laboratory, Electronics Command, Fort Monmouth, N.J., as directed by the Army Materiel Command, provided a weather radar team on Barbados to obtain quantitative estimates of precipitation and storm characteristics for aircraft mission planning and time-lapse photography of the offcenter scope to study the origin, development, movement, size, and intensity of tropical weather disturbances within the range of the radar. An AN/MPS-34 van-mounted weather radar, two U.S. Army power generators, and auxiliary equipment were used, located on Hackleton's Cliff near the east coast of the island approximately 104 km from the western section of the perimeter of the BOMEX square and 154 km from the NOAA ship *Mt. Mitchell,* which was positioned at the southwest corner of the BOMEX fixed-ship array. The antenna elevation at approximately 285 m above mean sea level extended the radar horizon. With the antenna elevation angle at about 0°, it was possible to detect many targets at ranges up to 350 km or greater. Characteristics of the AN/MPS-34 radar are listed in table 2.

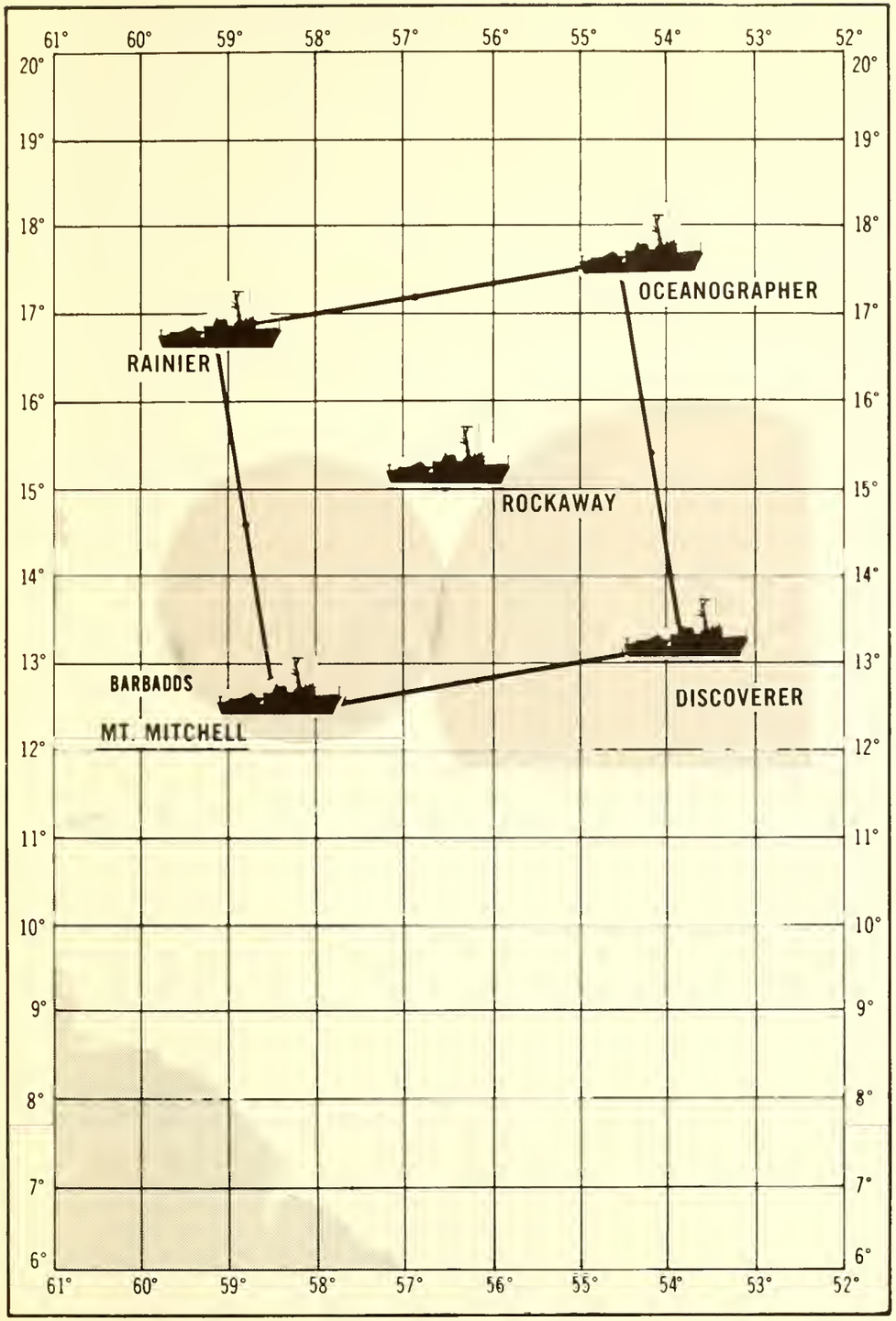

Figure 1. BOMEX fixed-ship array.

Table 1. Dates and times of data products selected

Date (1969)	Surface radar composite (GMT)	Aircraft radar and flight track mosaic (GMT)	ATS III satellite photograph (GMT)	HRIR contour map (GMT)	MRIR contour map (GMT)
June 20	1125 1615 2030		1118 1608 2029		
June 21	0308 1114 1445 2030	1319-1628	1117 1618 2029	0308	0308 1456
June 22	0225 1015 1630 2030	1307-1601	1055 1632 2025		
June 23	0340 1111 1614 2030	1418-1639	1118 1611 2030	0328	0329
June 24	0241 1125 1305 2158	1315-1623	1117 1610 2043	0244	1432
June 25	0356 0951 1547 2020	1316-1626	1109 1608 2035	0348	
June 26	0251 1014 1616 2014		1117 1615 2035		0305 1452
June 27	0435 1252 1605 2029		1254 1605 2028		
June 28	0329 1057 1602 2021	1327-1627	1108 1614 2020	0324	1512
June 29	0232 1122 1558 2038	1319-1630	1119 1706 2040		1430
June 30	0349 1120 1623 2020	1307-1612	1110 1625 2033	0344	0345 1532
July 1	0340 1122 1614 2031		1120 1609		0301
July 2	0329 1116		1121 1555 2036		

Fifty-eight 30-m rolls of 35-mm film containing photographs of the radar plan-position indicator (PPI) scope were obtained. A gain-step system to reduce receiver gain was used to acquire quantitative information about storm intensities. The system had six gain levels, calibrated to yield minimum detectable signal at the first level, a 19-dB step to level two, 18-dB steps to levels three, four, and five, and a 6-dB step to level six. Gainstep increments were checked for each new roll of 35-mm film and were recalibrated if any step had drifted more than 2 dB. The observed gain steppings were recorded in a logbook. The procedure for calibrating both gain steps and film provided a photographic record of minimum detectable signal at each of the gain settings.

The radar film is documented in "Weather Radar Investigations on the BOMEX," a report by Michael D. Hudlow, who served as project scientist for the radar team on Barbados. The report contains a quality review of each reel, and describes operational and calibration procedures, results of gain-step and film calibration, and automatic camera settings for each mode of operation. It also includes other significant information for film interpretation. Listed as *Research and Development Technical Report ECOM-3329*, the document is available from the National Technical Information Service, U.S. Department of Commerce, Sills Building, 5285 Port Royal Road, Springfield, Va. 22151.

The other surface weather radar data were obtained aboard the NOAA ship *Discoverer,* stationed at the southeast corner of the BOMEX fixed-ship array, by a Selenia radar, Model Meteor 200RNT-2S, whenever this radar was not being used for rawinsonde balloon tracking. Characteristics of the radar are given in table 3.

During weather surveillance, 35-mm photographs were taken of a PPI display on a Navy VD-2 repeater scope displaying maximum ranges up to 360 km. The photographs were taken every 12 scans for 12-s one-scan exposures (complete 360° rotation of the radar antenna). With the antenna tilt angle held at 0°, the receiver gain was attenuated in calibrated steps. The first step was 15 dB; the remaining steps were 6 dB. Following the gain sequence, the antenna was tilted in 1° or 2° steps at normal receiver gain until all echoes had disappeared. At the conclusion of the

Table 2. Island radar characteristics

Characteristics	Nominal value
Transmitted power	180 kw (peak)
Wavelength	3.2 cm
Antenna shape/diameter	Parabolic/2.4 m
Horizontal beam width	1°
Vertical beam width	1°
Antenna rotation rate	5 rpm
Minimum detectable signal	—105 dBm
Pulse repetition rate	186 pps
Pulse width	5×10^{-6} s
Range units	Statute miles
Sensitivity time control	Off

Table 3. Discoverer radar characteristics

Characteristics	Nominal value
Transmitted power	175 kw (peak)
Wavelength	3.2 cm
Antenna shape/diameter	Parabolic/1.4 m
Horizontal beam width	1.25°
Vertical beam width	1.25°
Antenna rotation rate	5 rpm
Minimum detectable signal	−97 dBm
Pulse repetition rate	240 ± 24 pps
Pulse width	3×10^{-6} s
Range units	Nautical miles
Sensitivity time control	On

elevation sequence the antenna was returned to 0°.

Both in the case of the island and *Discoverer* radars, selection for this atlas was made from 35-mm photographs taken at 0° tilt and normal receiver gain setting.

As noted in the introduction, reproduction of the BOMEX square at exactly the same scale presented some problems. The individual radar echo information was collected as 35-mm photographs of the PPI display on a cathode ray tube. The surface-based radar composites were produced from enlargements of the island and *Discoverer* radar microfilm. Unfortunately, the two enlargement factors could not be made identical because of a finite number of enlargement options. On the average, the discrepancy between the two scale factors was less than 10 percent, and in preparing the composites the length of the sides of the BOMEX square was therefore determined by averaging the two scale factors.

Also taken into account here is the actual position of the *Discoverer*. At the beginning of BOMEX, the five ships at the corner and in the center of the array were fixed in position by means of deep-sea moorings. In the early part of the field operations, however, the mooring systems failed, and in processing the BOMEX data it became necessary to renavigate ship positions. The renavigation is reflected in the surface radar composites by displacement of the *Discoverer* radar center from the southeast corner of the array. The renavigated positions were obtained from the ship's logs and were checked against those calculated for inclusion in the BOMEX Ship Operations and Navigation Data Set placed in the BOMEX Permanent Archive. It is estimated that the renavigation is accurate within about 10 km.

AIRBORNE RADAR MOSAICS

The photographs included in the airborne radar mosaics were collected by a Sperry Gyroscope Co. AN/APN-59B radar carried aboard an Air Force Weather Service WB-47 aircraft flying at an altitude of approximately 9 km along the track shown in figure 2. Stationed at Ramey Air Force Base, P.R., the aircraft normally passed over Barbados en route to the BOMEX area. On some photographs, the island is visible as a ground pattern.

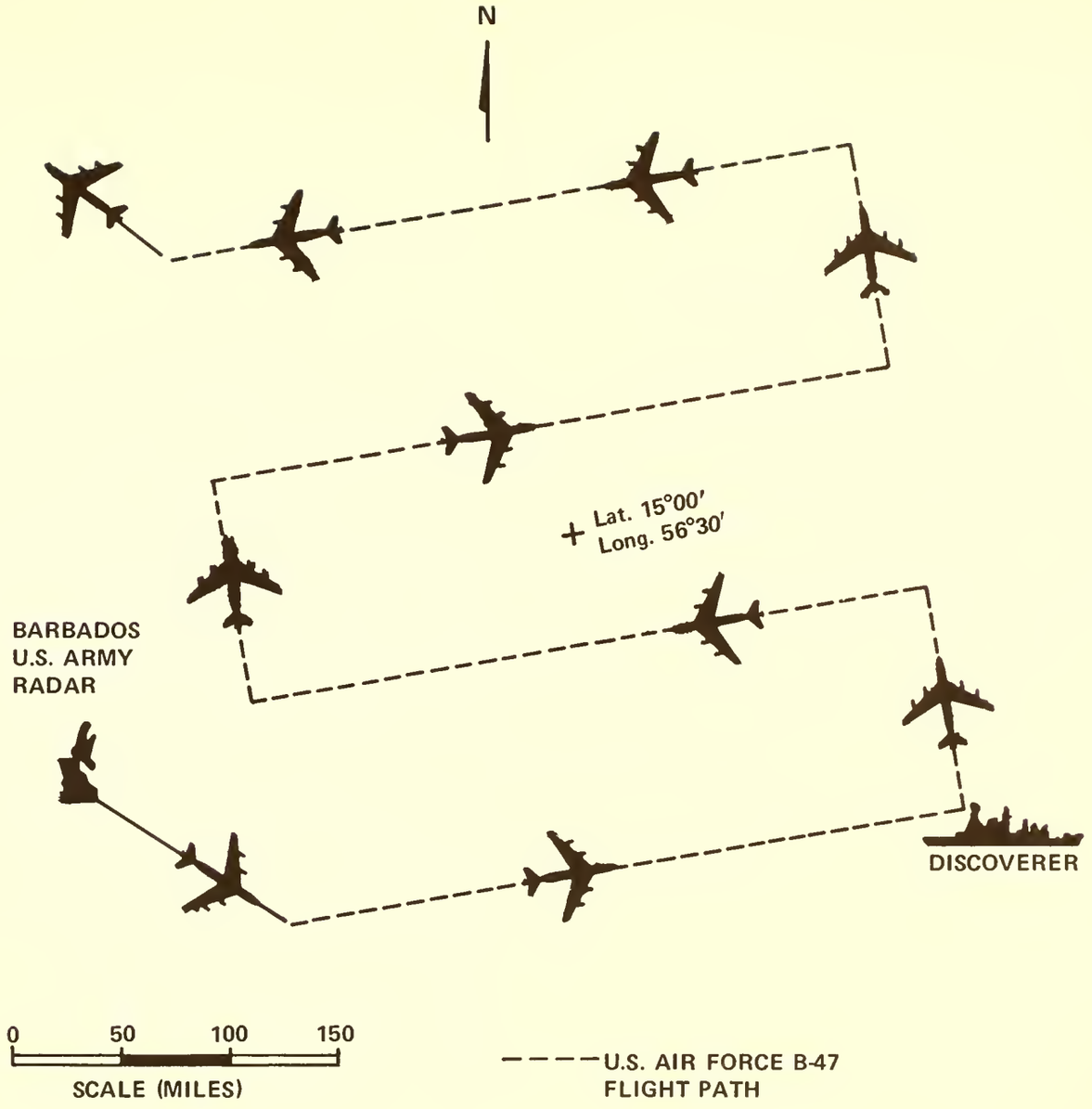

Figure 2. WB-47 aircraft flight track.

A small, lightweight, X-band (3 cm) system, the AN/APN-59B is designed to operate as a navigational and search radar, a weather radar, or a racon (beacon) interrogator-receiver. The indicator presentation is a 12.7-cm plan-position indicator (PPI) display. Five range displays are available: 6 to 60 km with 2-km and 10-km range markers; 100 km with 20-km range markers; 200 km with 40-km range markers; and 420 km with 60-km range markers. The start of the 6- to 60-km range display can be delayed any distance between 30 km and 400 km in order to expand any desired portion of the longer range presentation. Characteristics of the radar are listed in table 4.

The guidelines specified for collection of radar photographs were: one exposure every 12 scans when precipitation echoes were detected, adjustment of the antenna tilt angle for maximum echo return, and the use of 100-km total range for the scope setting. However, maximum ranges other than 100 km were used occasionally. When the range settings were uncertain for a reel of film, they could be verified in some instances from ground patterns of the island of Barbados. The bearing marker appearing on the radar scope indicates the aircraft heading with respect to true north, under the assumption that proper synchronization and calibration were maintained.

The mosaics were prepared by locating a particular radar photograph along the flight path and checking the flight path and the positions along it against aircraft navigation logs and flight track maps. By comparing the radar clock and the clock times recorded in the logs, particularly during aircraft turns, it was found that the radar clock was sometimes incorrect. This error was corrected and linearly distributed over the straight portions of the flight track. Individual photographs were then positioned at these corrected locations along the track and rotated so as to properly indicate aircraft heading. However, the aircraft radar photographs should be used only as qualitative indicators because of the lack of sensitivity and poor resolution of the AN/APN-59B radar.

Table 4. Airborne radar characteristics

Characteristics	Nominal value
Peak power	50 kw
Wavelength	3 cm
Horizontal beam width	3.5°
Vertical beam width	5°
Beam tilt	From 10° up to 15° down
Pulse length	100 m or 1,350 m
Pulse repetition frequency	180 pps (long pulse) 1,025 pps (short pulse)
PPI scan	360° clockwise at 11 to 16 or 49 ± 7 rpm; speed automatically determined by range and function
Antenna reflector stabilization	
Pitch	From 12° (nose down) to 15° (nose up)
Roll	±30°
Azimuth reference	Relative to true north

SATELLITE DATA

ATS III Satellite Photographs

ATS III was launched from the Air Force Eastern Test Range, Cape Kennedy, Fla., on November 5, 1967. The satellite achieved a 24-hr geosynchronous orbit at an altitude of about 35,515 km. This nearly circular orbit combined with the earth's rotational period of 24 hr makes the satellite appear to hover over a fixed geographic point on the Equator. The satellite

rotates about its spin axis aligned with the earth's axis at nominally 100 rpm. Unless moved by command, it remains above a point very close to the Equator where it can observe the full disc of the earth. During May 1969 ATS III was located above the Equator at 73° W. Subsequently, the satellite was moved progressively eastward toward the BOMEX array, reaching 47° W on July 2, 1969, and its position stabilized at about 46° W during July. The movement of the subsatellite point during May, June, and July 1969 is presented in figure 3.

The ATS III photographs included in this atlas were obtained by the Multicolor Spin Scan Cloud Camera (MSSCC), on board the satellite. The main components of the MSSCC are a high-resolution telescope with a small field of view (4 km at the subsatellite point), three photomultiplier light detectors, and a precision latitude step mechanism. The three spectral bandpasses of the optical system defined by optical filters and photocathodes are: Channel 1, 3800 A to 4800 A (blue); Channel 2, 4800 A to 5800 A (green); and Channel 3, 5500 A to 6300 A (red). The latitude step motion combined with the spinning motion permits the satellite to scan a complete earth disc with 2,400 horizontal, west-to-east, scan lines in 24 min.

The ATS III meteorological data are processed by the Electronic Image System (EIS) photofacsimile recorder, which displays the video information on a high-resolution 12.7-cm cathode ray tube for projection onto Ektacolor, type S negative, or Polaroid, type 55 P/N, film. A gray-scale display is added to all recorded photofacsimile appearing as a 0.3-cm vertical bar at the right edge of a picture. The bar consists of 10 levels of gray, from black at the top step to white at the 10th step. Each step is equivalent to 192 lines and 127 picture element pulses. No calibrated gray-scale information was retained for the atlas displays.

The characteristics of the ATS III satellite and its data collection system are summarized in *The User's Guide to ATS III Meteorological Data,* published by the Goddard Space Flight Center, NASA, Greenbelt, Md. 20771. Selected full-disc and synoptic-scale ATS III satellite photographs for the entire duration of BOMEX appear in *BOMEX Atlas of Satellite Cloud Photographs* by Vance A. Myers, Barbados Oceanographic and Meteorological Analysis Project Office, National Oceanic and Atmospheric Administration, Rockville, Md. 20852.

The MSSCC pictures are not gridded automatically. Separate latitude-longitude grids, including key geographical outlines, are computer generated and subsequently exposed to transparent film.

Grid fit is usually better than 1° of great circle arc in the region of the subsatellite point and 3° of arc near the horizon. Gridding accuracy on the order of 10 to 20 km can be attained in localized areas where coastlines or conspicuous land masses are visible in the picture.

The enlargements of the BOMEX area from the ATS III photographs were gridded by the Photographic Laboratory, Nimbus and ATS Data Utilization Center, Goddard Space Flight Center. The gridding of the enlargements was checked against the Windward Islands and the coastline of South America. Grid displacements, without rotation, are indicated in this atlas, giving the direction toward which the BOMEX grid is to be shifted and the amount of the displacement.

Nimbus 3 Satellite Cloud Maps

Nimbus 3 was launched into a nearly circular orbit from the Western Test Range at Vandenburg Air Force Base, Calif., on April 14, 1969. The satellite achieved a sun-synchronous orbit at an altitude of about 1,110 km with a period of 107 min. The satellite contains an active three-axis stabilization system that maintains the spacecraft body axes earth stabilized. The yaw axis points normal to the earth, and a roll axis is aligned with the spacecraft velocity vector. All data obtained are mapped by using the orbit ephemeris data; attitude corrections are not included in the procedures for geographic location.

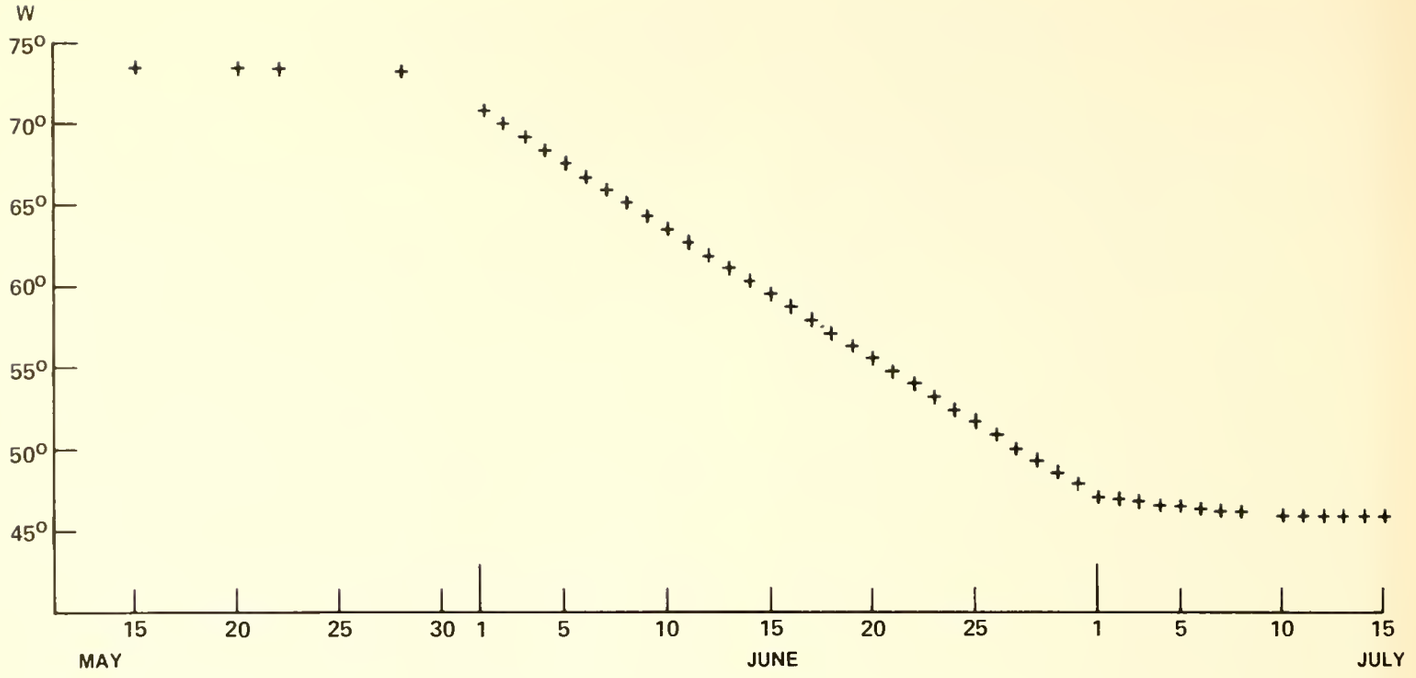

Figure 3. Movement of ATS III subsatellite point.

The HRIR cloud top maps presented in this atlas were derived from the nighttime data collected at nominally 0330 GMT in the 3.4- to 4.2-μ near-infrared region over the BOMEX area. The HRIR optical system consists of a scan mirror inclined 45° to the axis of rotation, which is coincident with the spacecraft velocity vector, a 10-cm f/1 modified Cassegrainian telescope, a chopper that interrupts the reflected radiation at the focus of the telescope, a reflective relay system that contains the dual bandpass filter, and an infrared detector.

At night the satellite travels southward, and the field of view scans across the earth from west to east. The instantaneous field of view at the subsatellite point is a square, 0.5° on a side, resulting in a ground resolution of 8.5 km. This resolution deteriorates as the scan moves sideways toward the horizon. For the BOMEX area the nadir angle was about 15°, with a ground resolution of about 10 km. Gridding accuracy is better than 1° of great arc.

The temperature data used were in the form of a Mercator projection at a scale of 1: 1,000,000 having one temperature data point every 0.125° of both latitude and longitude over the BOMEX area, 10° to 20° N, 50° to 60° W. These data were provided by Goddard Space Flight Center, NASA, in computer printout form.

By assuming that the cloud tops have the same temperature as the surrounding air, a minimum cloud height can be inferred by comparing equivalent blackbody temperatures with temperature-pressure-moisture soundings taken above each of the five BOMEX ships every 1½ hr. Once the pressure-temperature relation is known, isobar maps of minimum cloud tops can be drawn over the BOMEX area. An average temperature pressure sounding for the area was obtained by averaging, in 100-mb pressure level steps, the temperatures from all soundings taken close to satellite passage time. This averaging procedure included the sea-surface pressure taken by all five ships.

The equivalent blackbody temperature radiation reaching the satellite sensor is attenuated due to absorption by the carbon dioxide and water vapor present in the atmosphere. Near the horizon the radiation has to travel through an increased amount of atmosphere, making the attenuation a function of scan angle. To take these factors into account, a correction formula was used, which is based on a model calculation and was derived by W. L. Smith, P. K. Rao, R. Koffler, and W. R. Curtis ("The Determination of Sea-Surface Temperature From Satellite High Resolution Infrared Window Radiation Measurements." *Monthly Weather Review*, Vol. 98, No. 8, 1970, pp. 604-611). If T_{BB} is the equivalent blackbody temperature in degrees Kelvin observed by the satellite, and θ is the nadir angle in degrees, then the corrected temperature T_C is given by:

$$T_C = T_{BB} + \left[a_0 + a_1 \left(\frac{\theta}{60}\right)^{a_2}\right] \cdot \ln\left(\frac{100}{310 - T_{BB}}\right)$$

$$(210^\circ\ \mathrm{K} \leq T_{BB} \leq 300^\circ\ \mathrm{K} \text{ and } \theta \leq 60^\circ),$$

where $a_0 = 1.13$, $a_1 = 0.82$, and $a_2 = 2.48$.

Under conditions of broken cloudiness due to the partial filling of the instantaneous field of view, the contamination of the cloud top temperature is such as to lead to a higher equivalent blackbody temperature, and thus the cloud height determined for such conditions constitutes a lower limit, i.e., a minimum cloud top height. Since some of the individual BOMEX soundings from which the average area sounding was obtained showed inversions below the 700-mb level, the average sounding, and therefore the cloud tops below 700 mb, must be used with caution.

The isopleth minimum cloud top height maps included in this atlas were hand contoured on the original unrenavigated Mercator data plots and labeled in a p* pressure system where $p^* = p_0 - p$, p(mb) = pressure aloft, and p_0 (mb) = sea-level pressure. The maps should not be construed as exact quantitative statements but rather as valuable qualitative indicators.

The MRIR cloud top maps were derived from both daytime and nighttime data collected at nominally 1500 and 0330 GMT, respectively. For the maps included here the electromagnetic radiation emitted and reflected from the earth and its atmosphere was measured in the atmospheric "window" channel (10 to 11 μ), which provides surface and near-surface temperatures over clear portions of the atmosphere and cloud cover and cloud height information during both day and night.

The radiant energy is collected by a flat scanning mirror inclined 45° to the optical axis. The mirror rotates at 9 rpm and scans in a plane perpendicular to the satellite velocity vector. The incident radiation is then focused onto a thermistor bolometer detector through appropriate optical filters. To obtain an a.c. signal from the detector, the energy is modulated by a mechanical chopper. This electrical signal is then amplified and demodulated to yield an analog output of 0 to −6.4 V, corresponding to the equivalent blackbody temperatures. The analog output is sampled 33⅓ times per second and converted to 8-bit digital data.

The angular field of view for the 10- to 11-μ channel is about 3°, resulting in a nominal spatial resolution of approximately 55 km at the subsatellite point. Gridding accuracy is better than 1° of great arc.

The equivalent blackbody temperature data from the MRIR were used in the form of a horizontal stereographic projection at a scale of 1: 4,000,000 and were specifically provided for this atlas by the Goddard Space Flight Center, NASA, in computer printout form. The isopleth maps were hand contoured on the uncorrected unrenavigated temperature fields and were not converted to height fields.

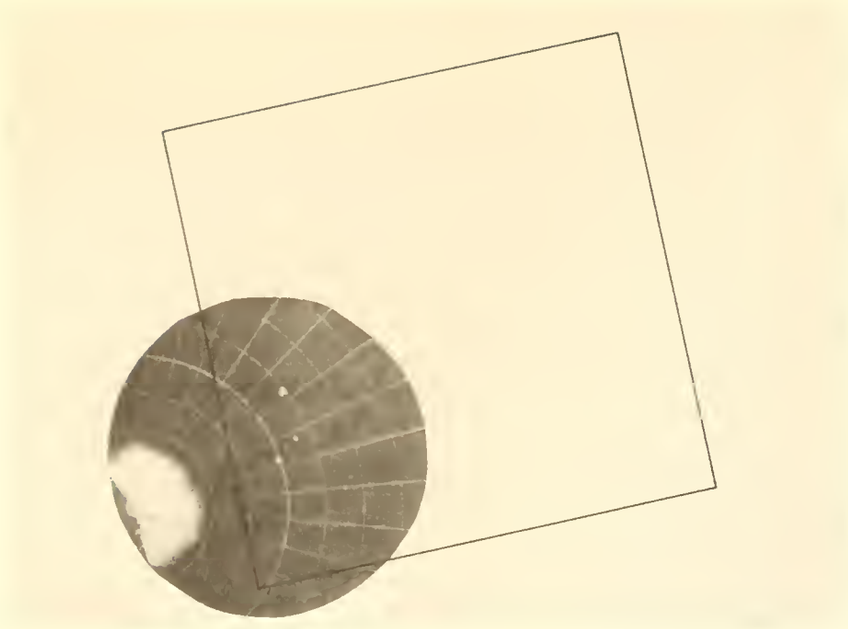

Surface radar composite, June 20, 1969, 1125 GMT.

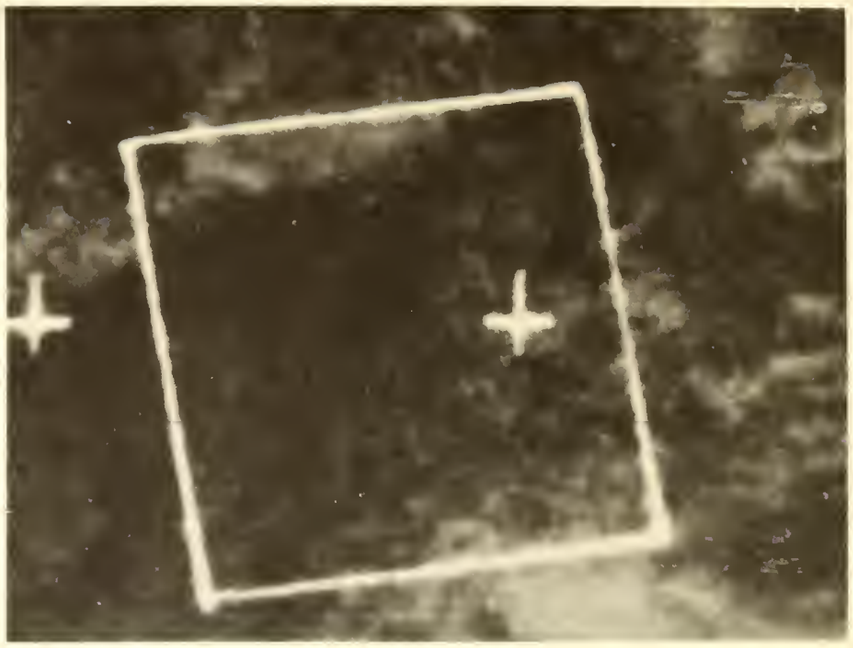

ATS III satellite photograph, June 20, 1969, 1118 GMT.
Displacement 65 km, 190°.

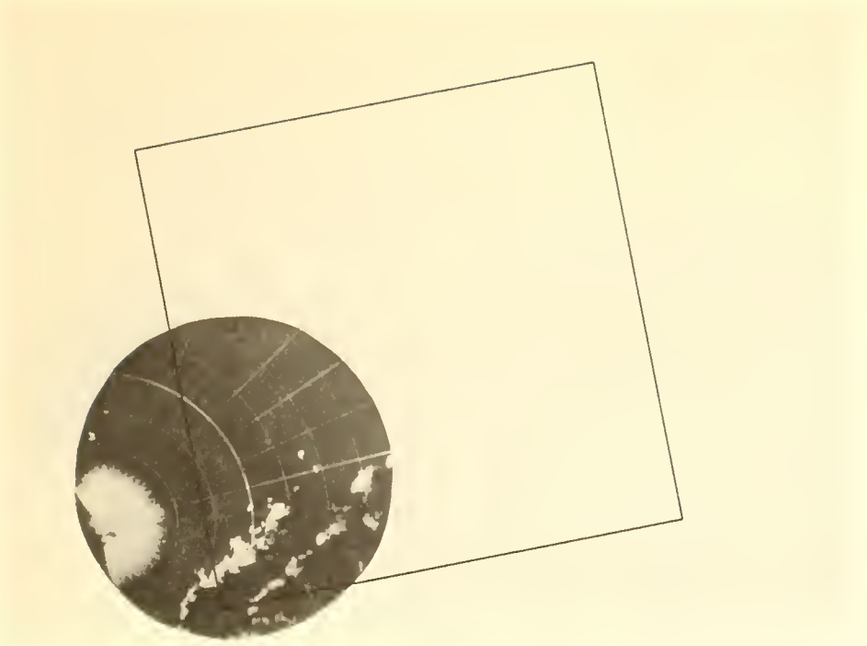

Surface radar composite, June 20, 1969, 1615 GMT.

ATS III satellite photograph, June 20, 1969, 1608 GMT.
Displacement 30 km, 210°.

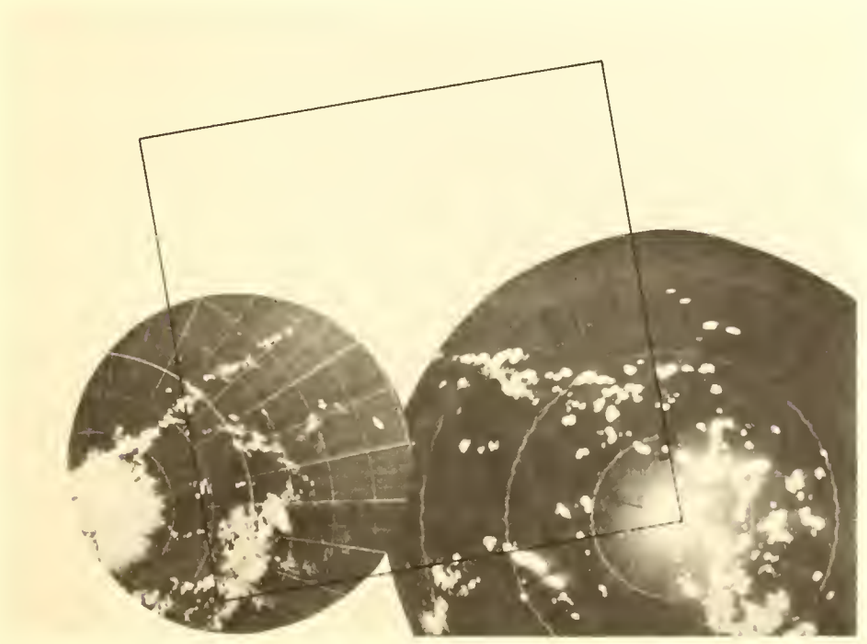

Surface radar composite, June 20, 1969, 2030 GMT.

ATS III satellite photograph, June 20, 1969, 2029 GMT.
Displacement 45 km, 220°.

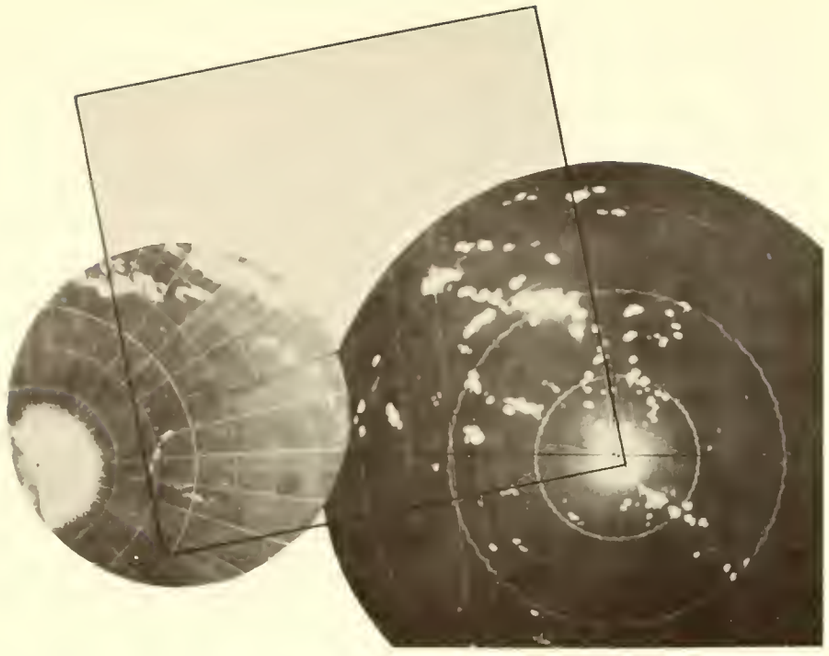

Surface radar composite, June 21, 1969, 0308 GMT.

Nimbus 3 HRIR cloud top contour map, June 21, 1969, 0308 GMT.

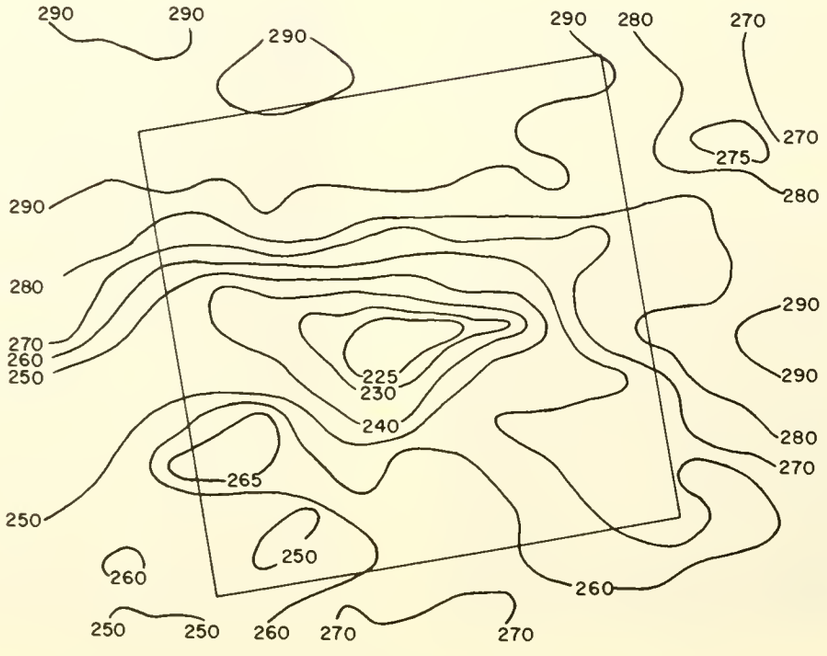

Nimbus 3 MRIR cloud top contour map, June 21, 1969, 0308 GMT.

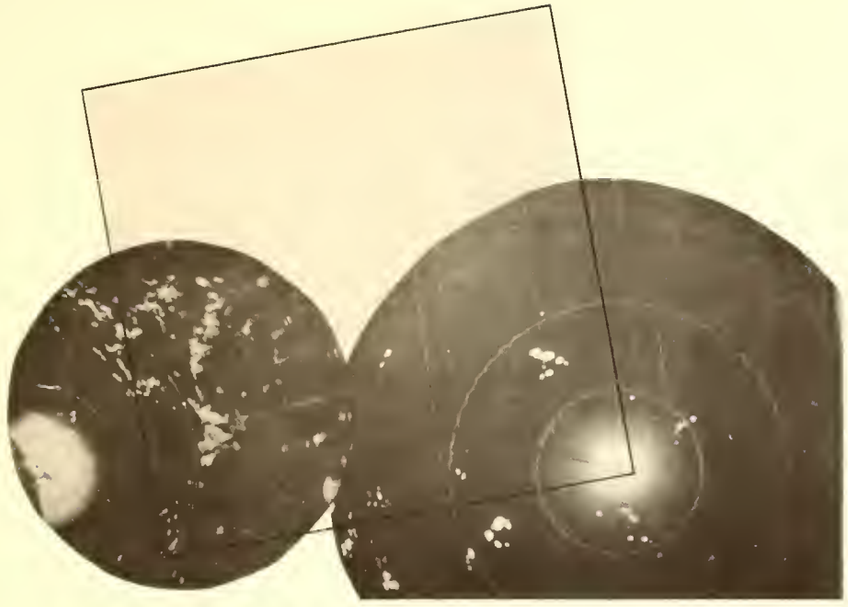

Surface radar composite, June 21, 1969, 1114 GMT.

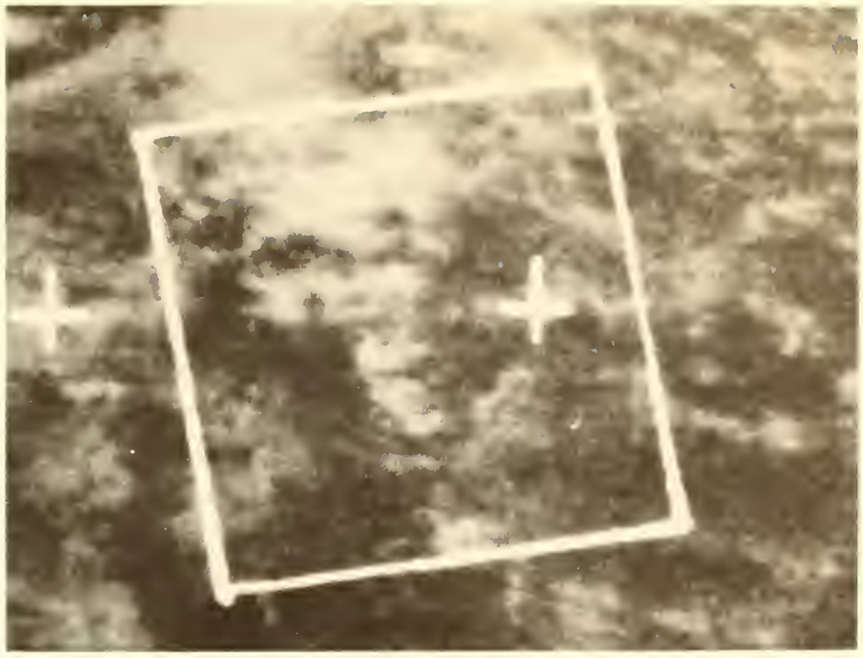

ATS III satellite photograph, June 21, 1969, 1117 GMT.
Displacement 40 km, 330°.

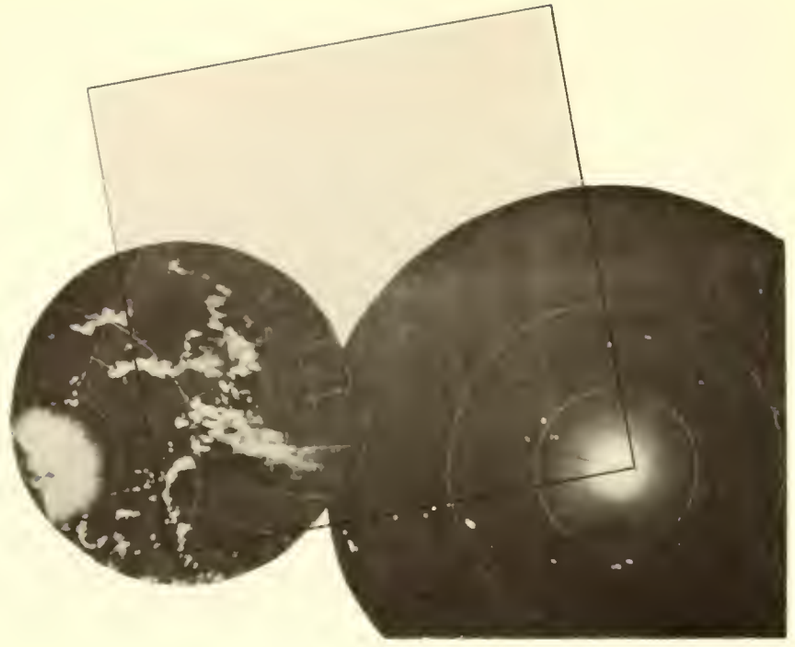

Surface radar composite, June 21, 1969, 1445 GMT.

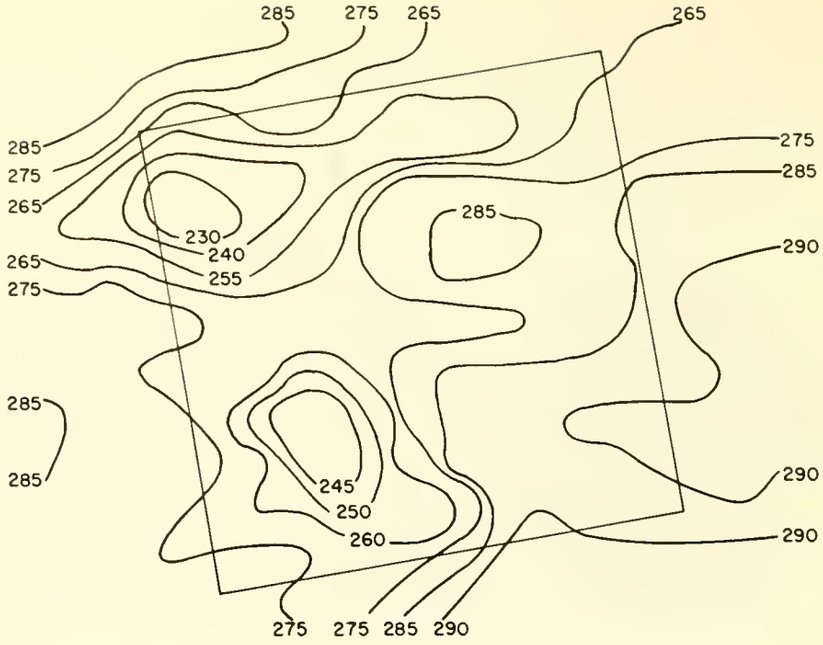

Nimbus 3 MRIR cloud top contour map, June 21, 1969, 1456 GMT.

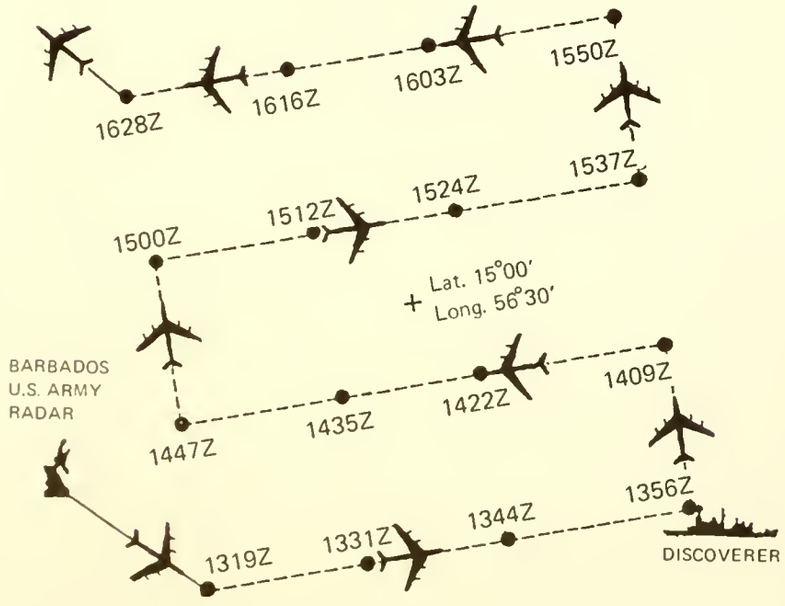

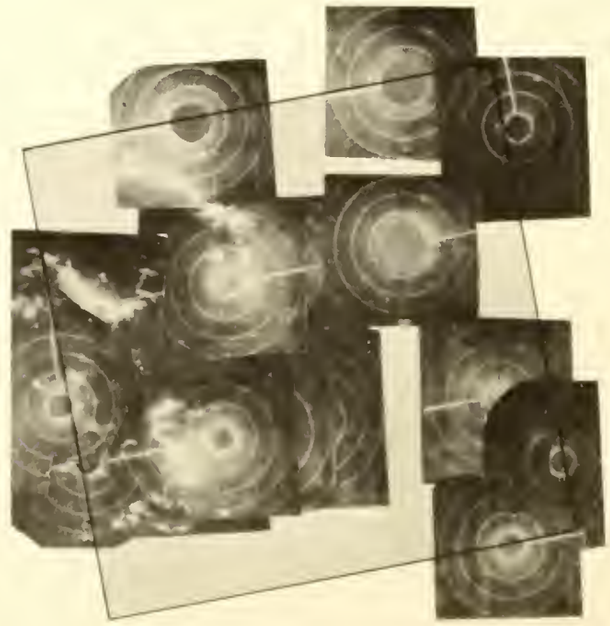

Aircraft flight track and radar mosaic, June 21, 1969, 1319-1628 GMT.

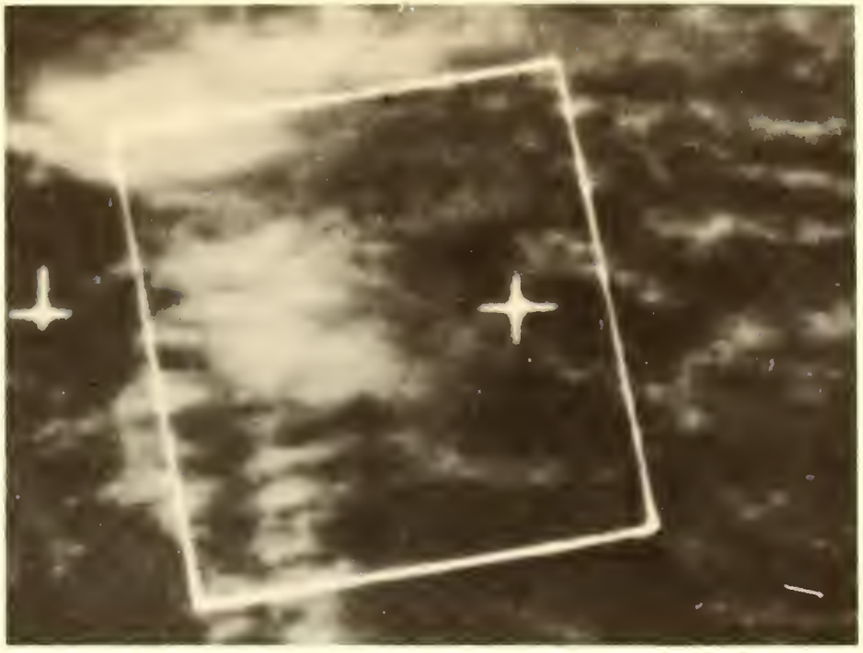

ATS III satellite photograph, June 21, 1969, 1618 GMT.
Displacement 110 km, 350°.

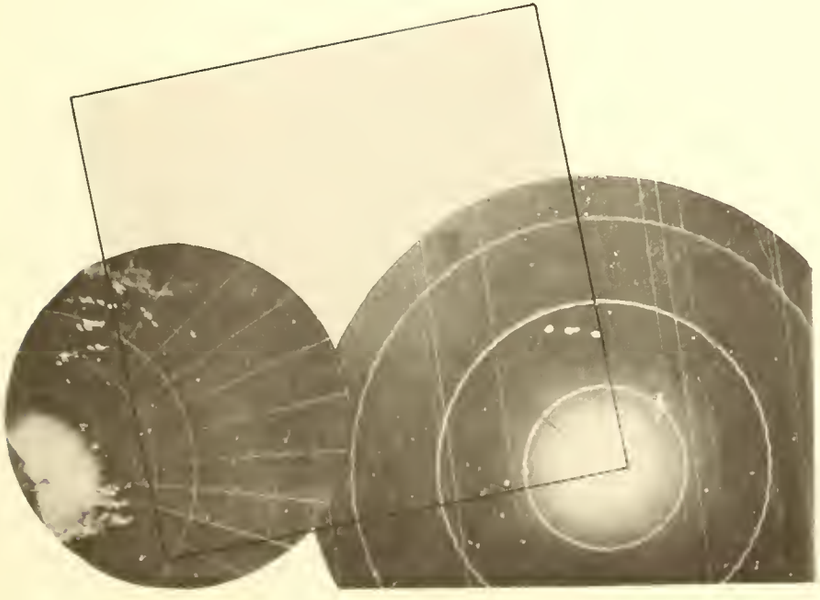

Surface radar composite, June 21, 1969, 2030 GMT.

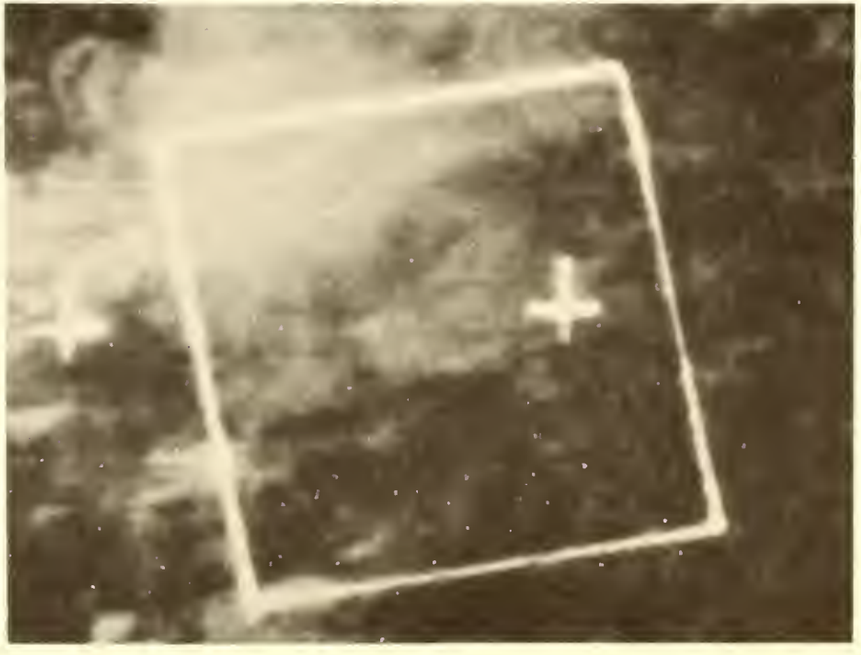

ATS III satellite photograph, June 21, 1969, 2029 GMT.
Displacement 90 km, 360°.

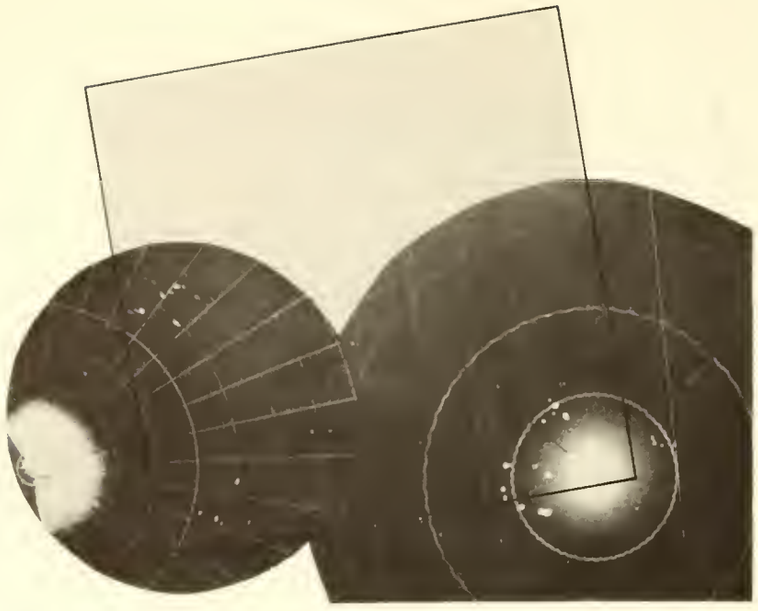

Surface radar composite, June 22, 1969, 0225 GMT.

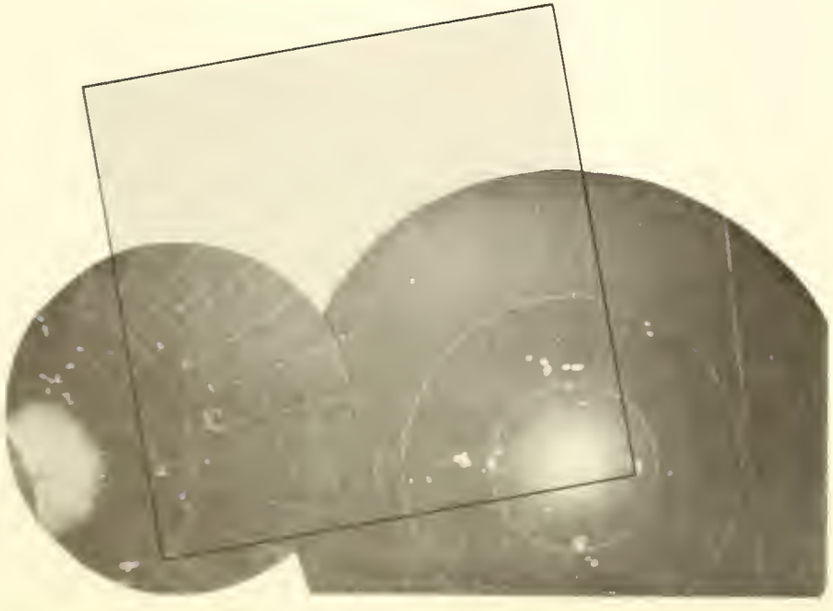

Surface radar composite, June 22, 1969, 1015 GMT.

ATS III satellite photograph, June 22, 1969, 1055 GMT.
Displacement 165 km, 130°.

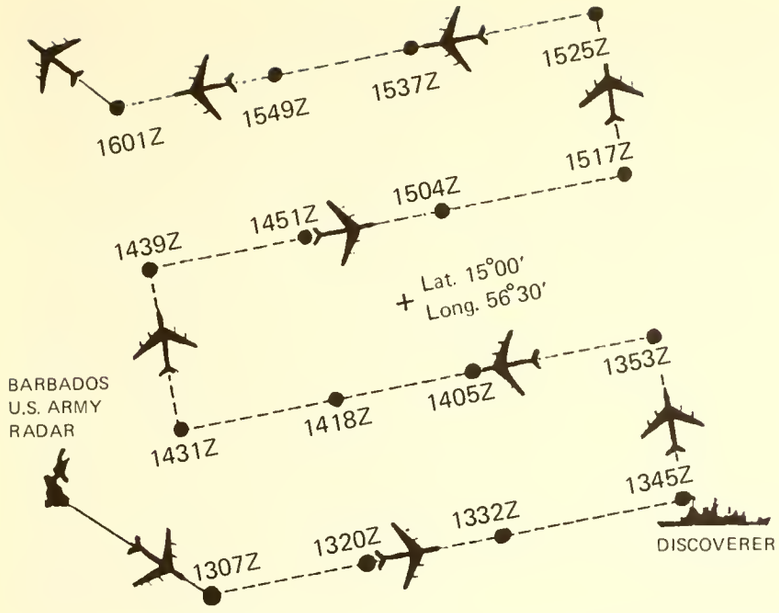

Aircraft flight track and radar mosaic, June 22, 1969, 1307-1601 GMT.

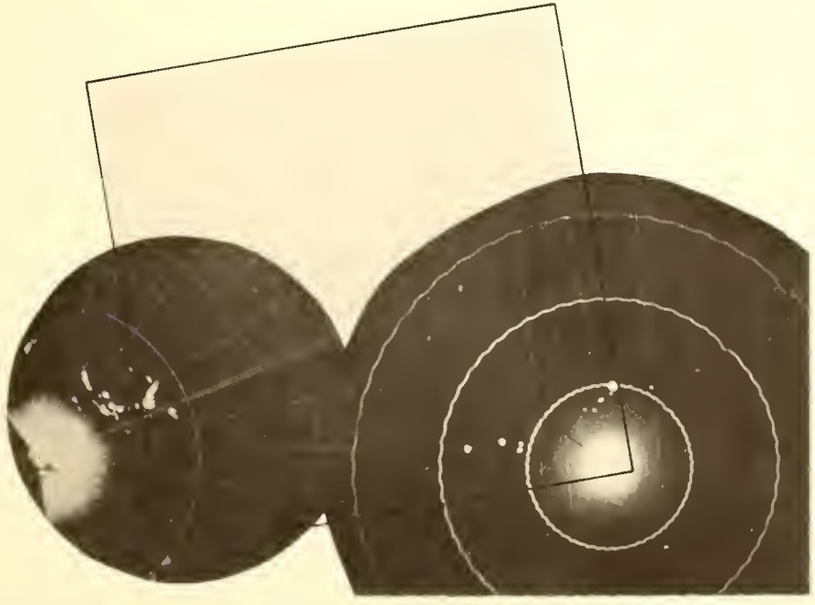

Surface radar composite, June 22, 1969, 1630 GMT.

ATS III satellite photograph, June 22, 1969, 1632 GMT.
No displacement.

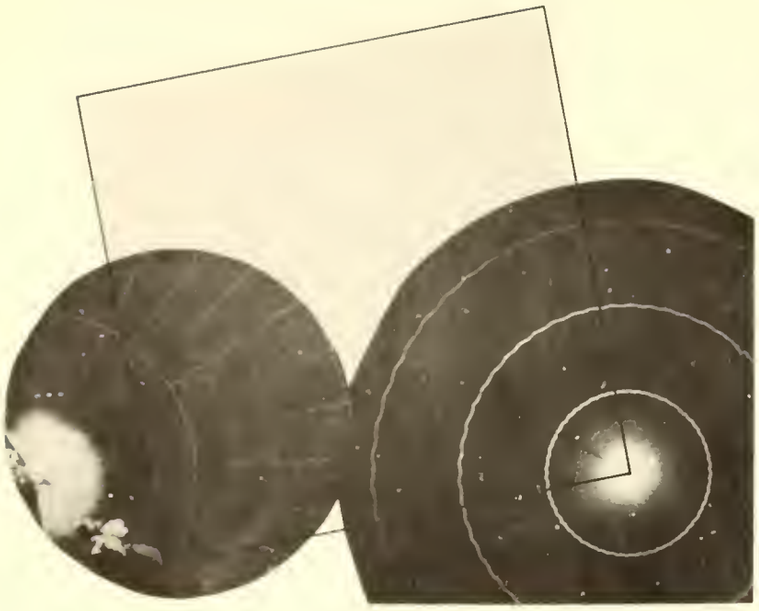

Surface radar composite, June 22, 1969, 2030 GMT.

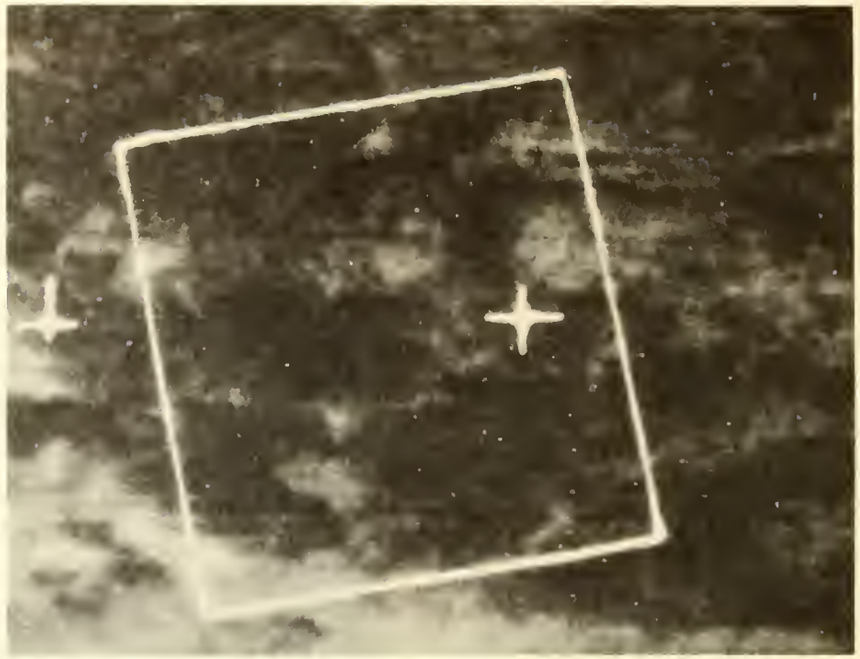

ATS III satellite photograph, June 22, 1969, 2025 GMT.
Displacement 40 km, 310°.

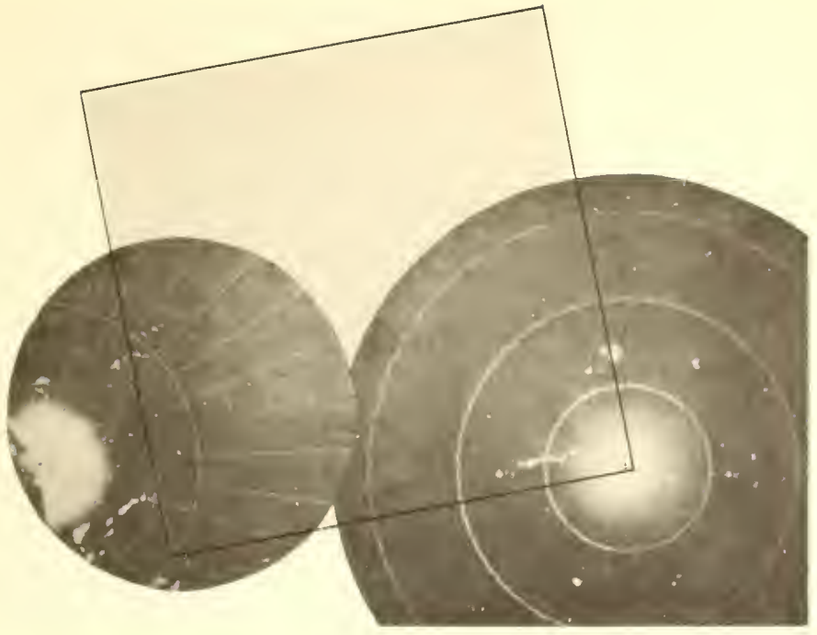

Surface radar composite, June 23, 1969, 0340 GMT.

Nimbus 3 HRIR cloud top contour map, June 23, 1969, 0328 GMT.

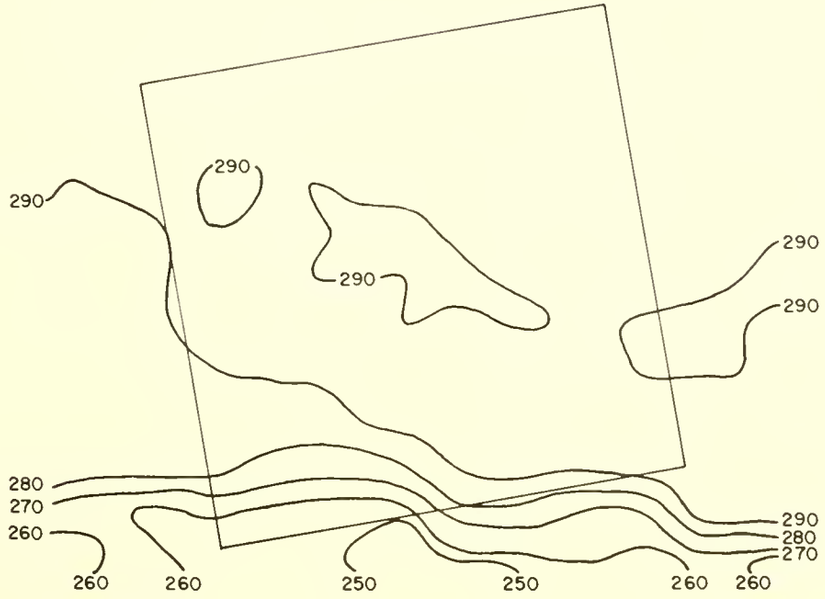

Nimbus 3 MRIR cloud top contour map, June 23, 1969, 0329 GMT.

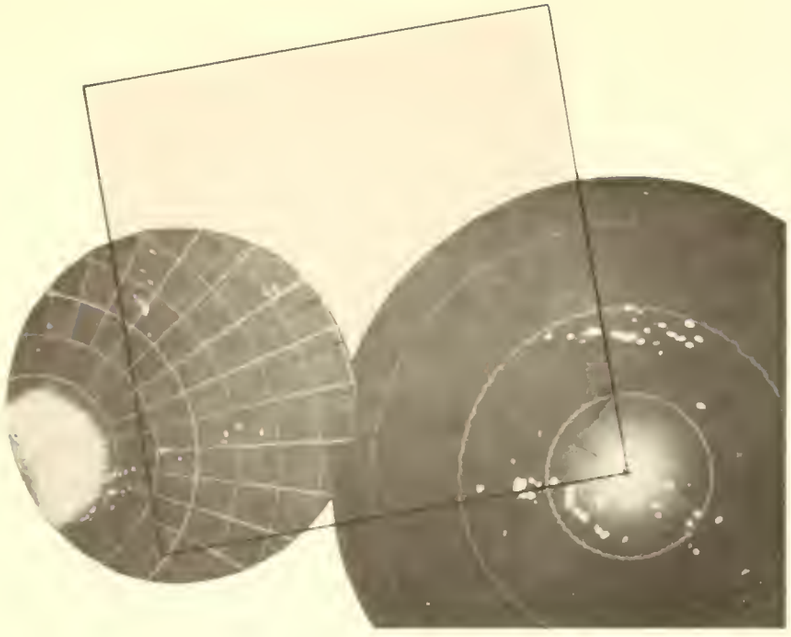

Surface radar composite, June 23, 1969, 1111 GMT.

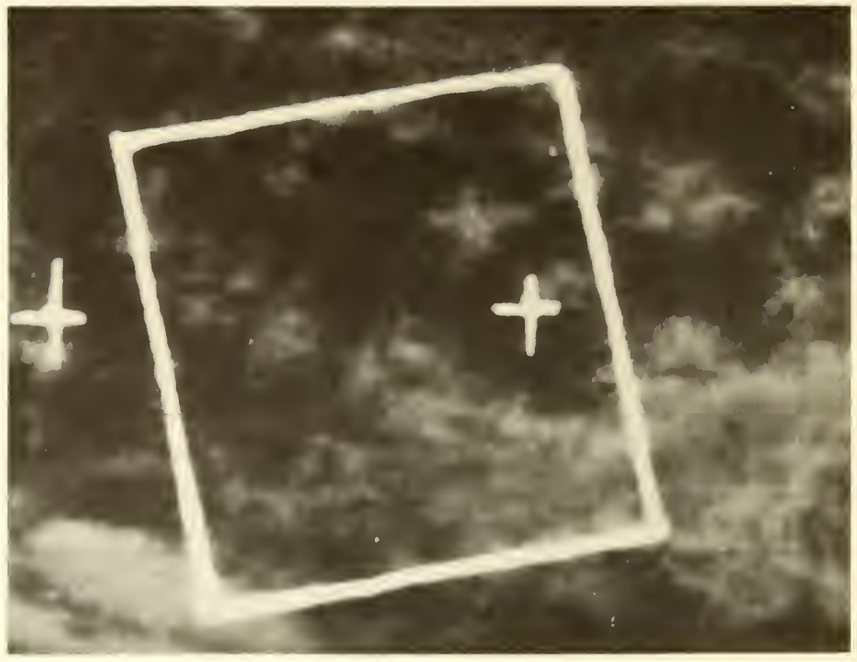

ATS III satellite photograph, June 23, 1969, 1118 GMT.
Displacement 110 km, 095°.

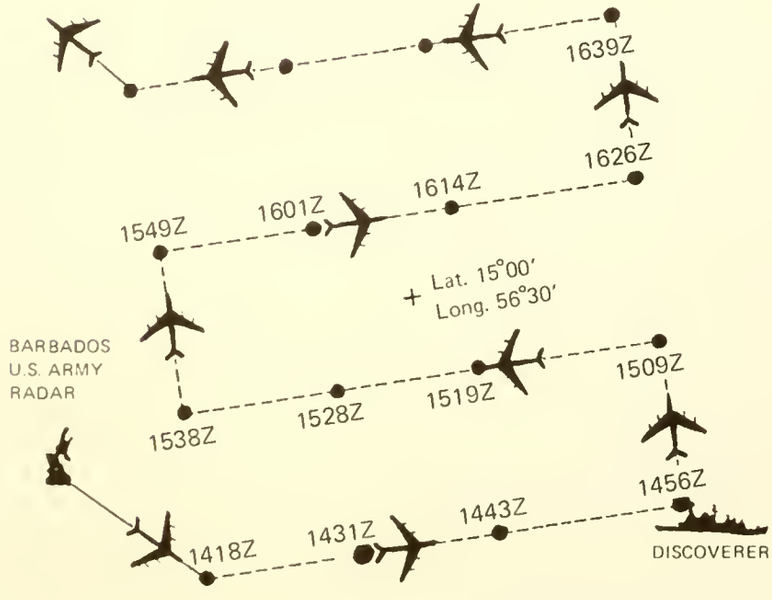

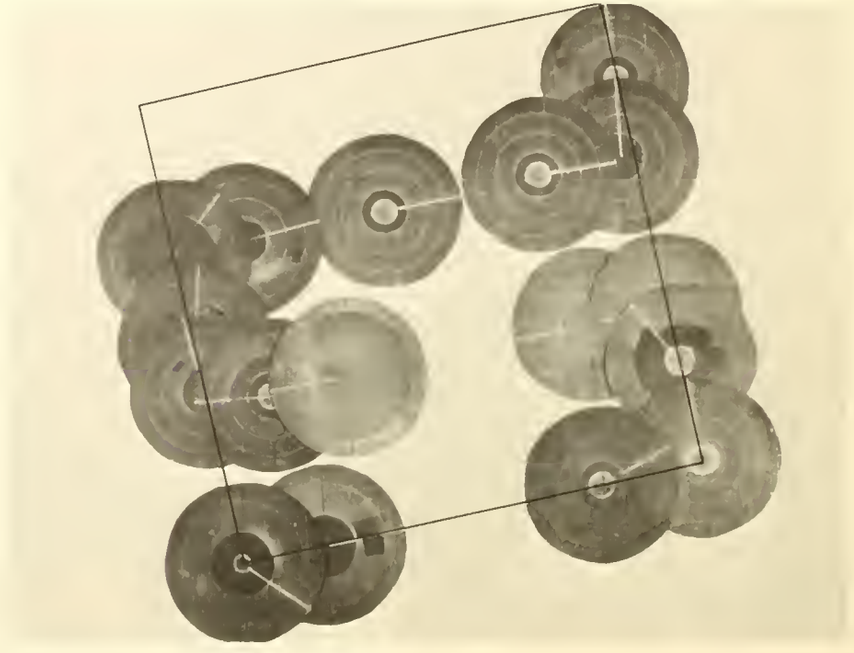

Aircraft flight track and radar mosaic, June 23, 1969, 1418-1639 GMT.

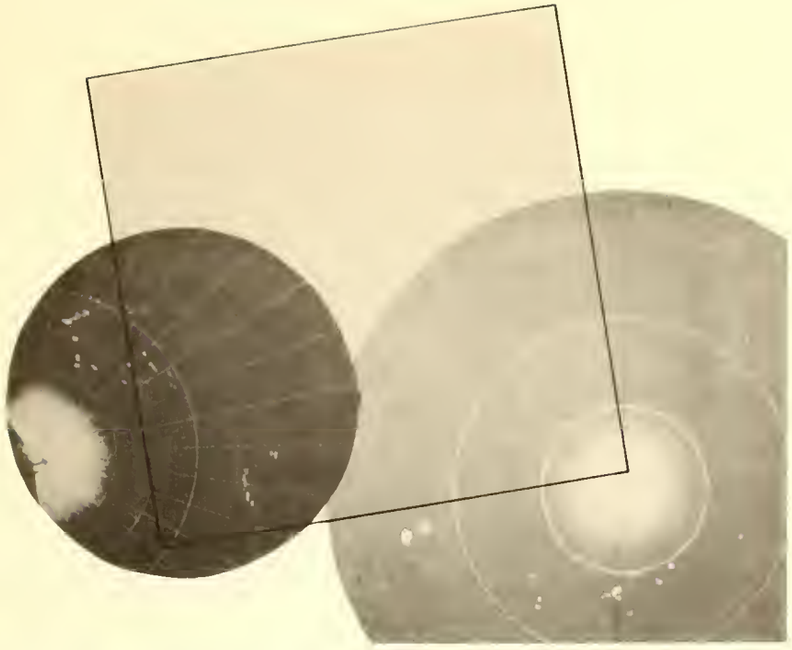

Surface radar composite, June 23, 1969, 1614 GMT.

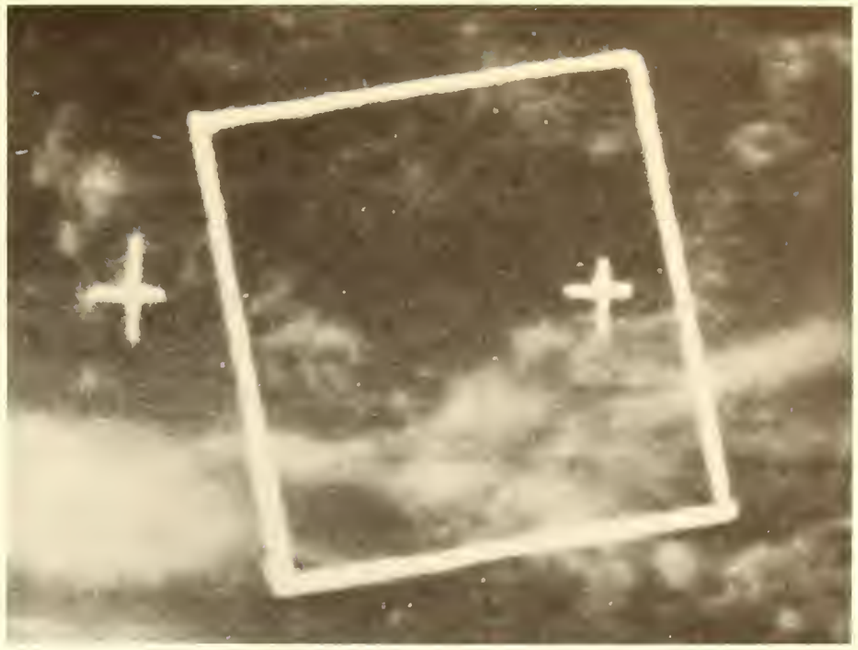

ATS III satellite photograph, June 23, 1969, 1611 GMT.
Displacement 85 km, 070°.

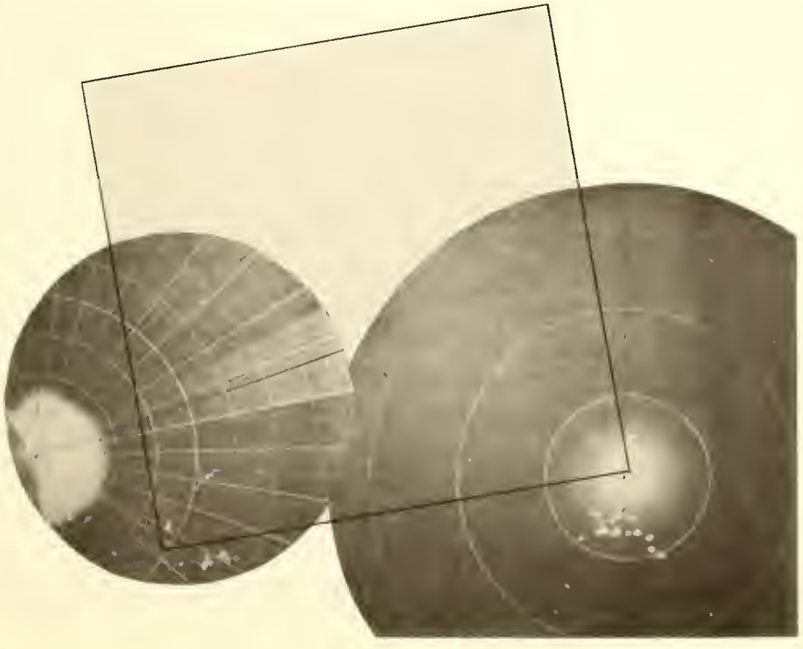

Surface radar composite, June 23, 1969, 2030 GMT.

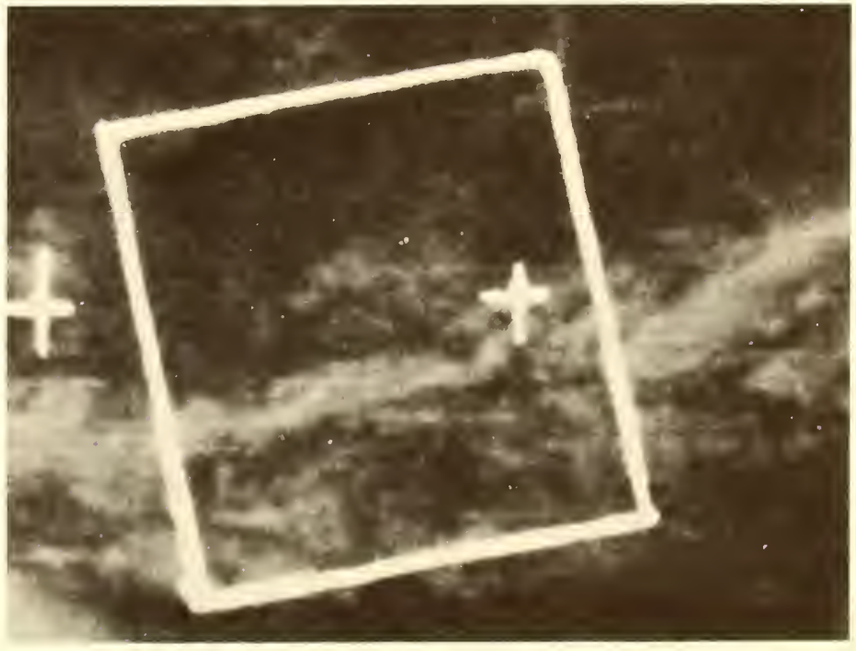

ATS III satellite photograph, June 23, 1969, 2030 GMT.
Displacement 85 km, 040°.

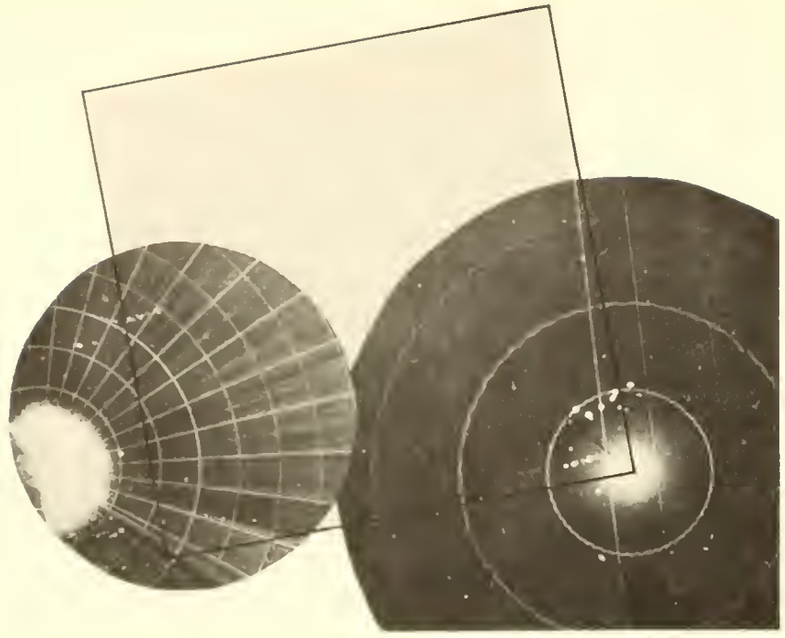

Surface radar composite, June 24, 1969, 0241 GMT.

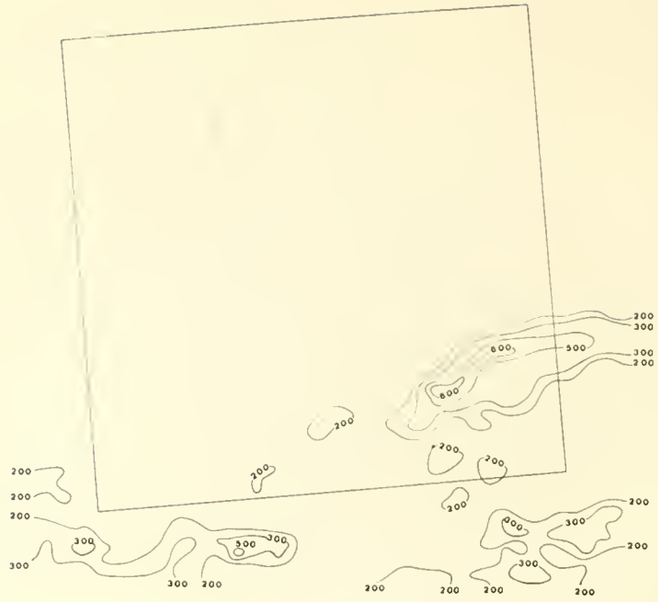

Nimbus 3 HRIR cloud top contour map, June 24, 1969, 0244 GMT.

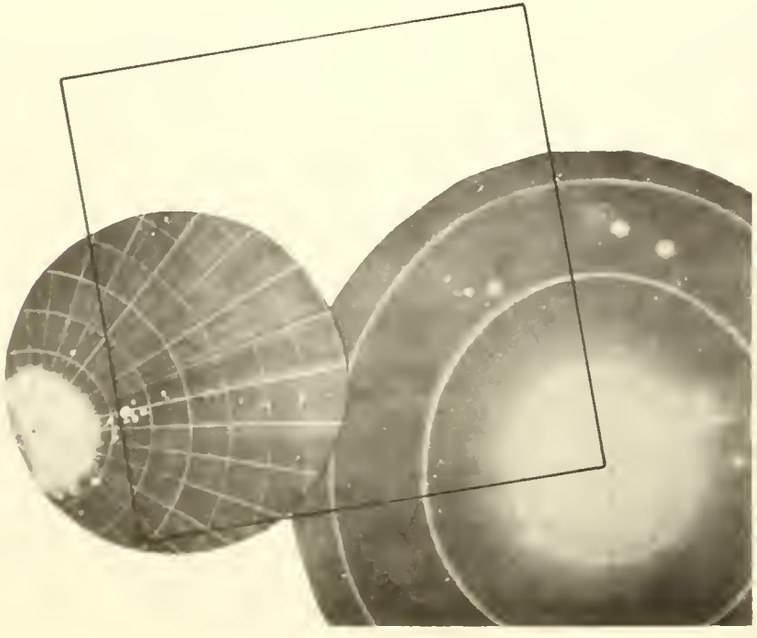

Surface radar composite, June 24, 1969, 1125 GMT.

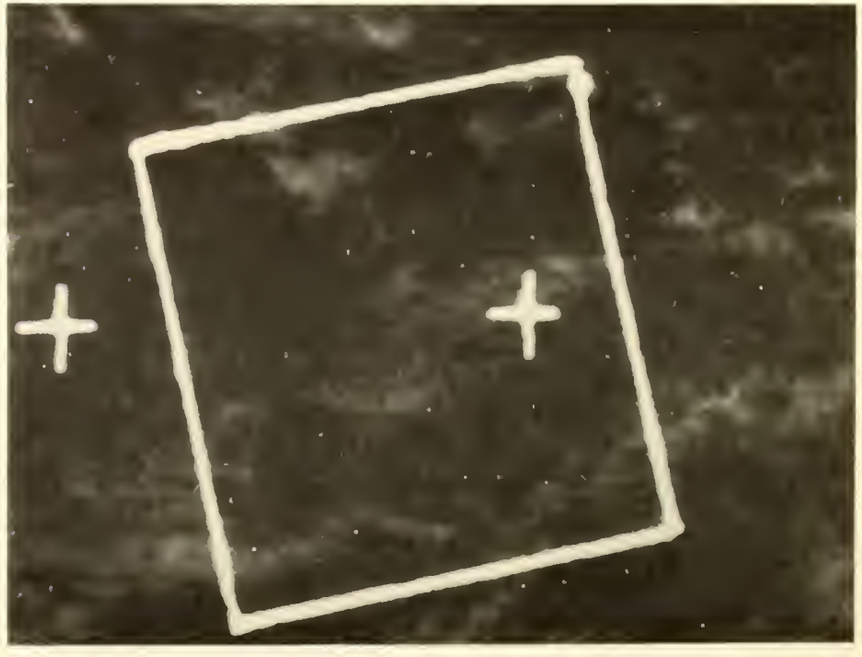

ATS III satellite photograph, June 24, 1969, 1117 GMT.
Displacement 100 km, 030°.

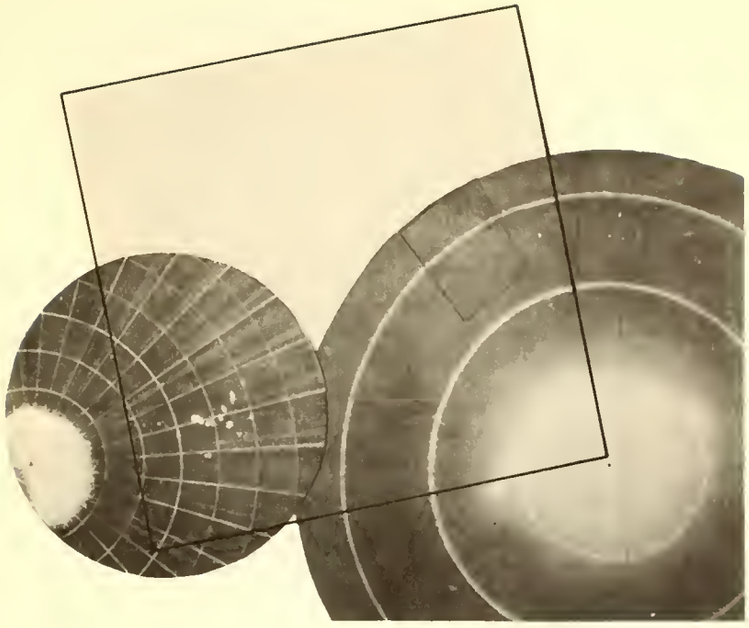

Surface radar composite, June 24, 1969, 1305 GMT.

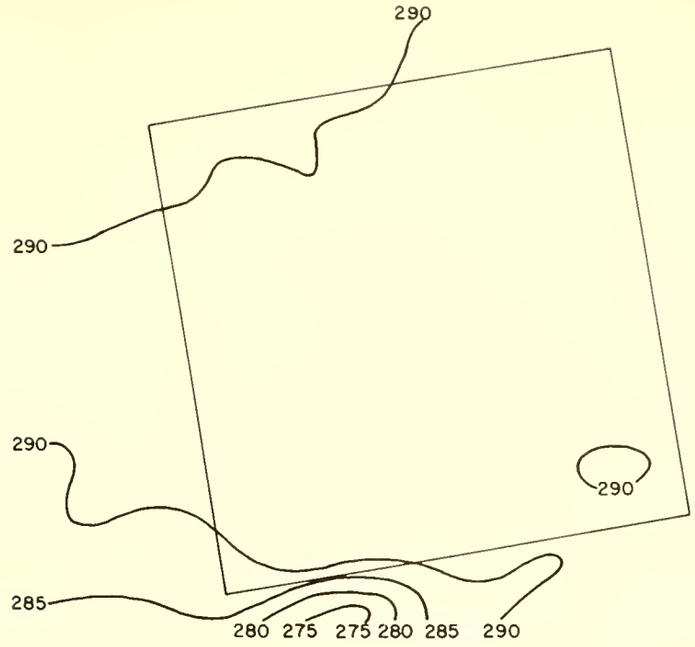

Nimbus 3 MRIR cloud top contour map, June 24, 1969, 1432 GMT.

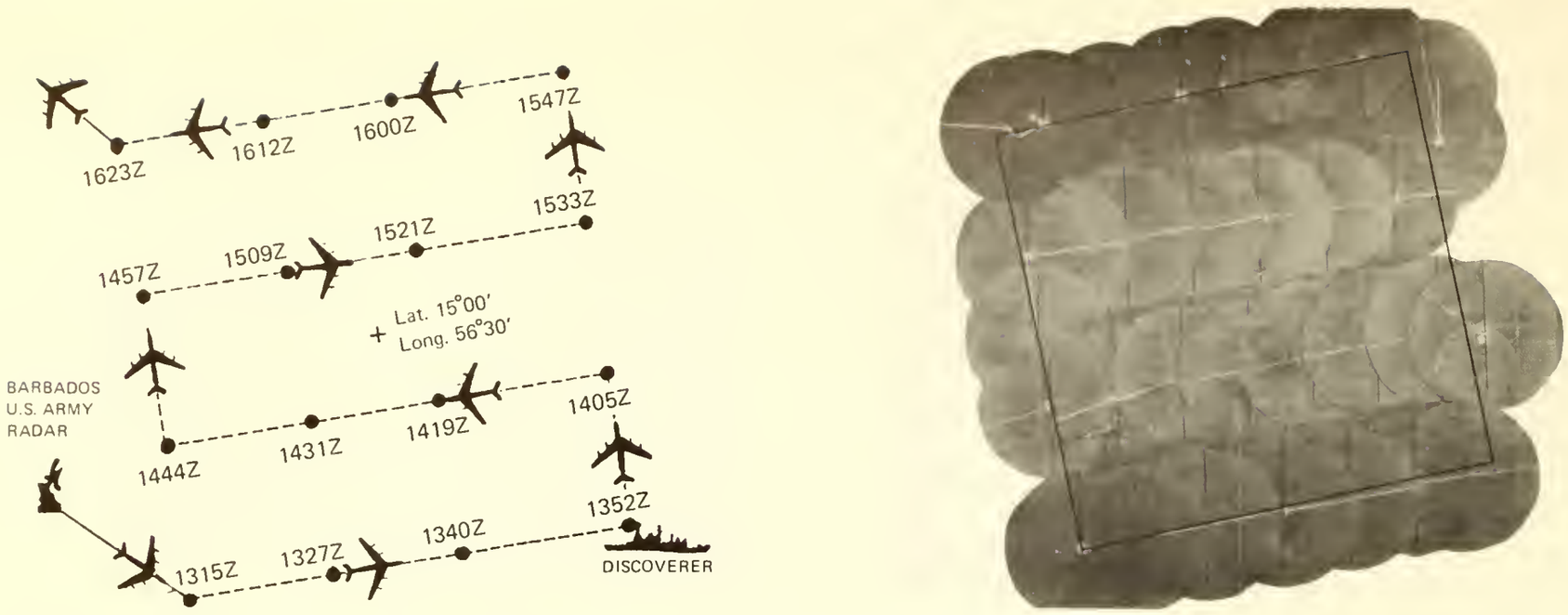

Aircraft flight track and radar mosaic, June 24, 1969, 1315-1623 GMT.

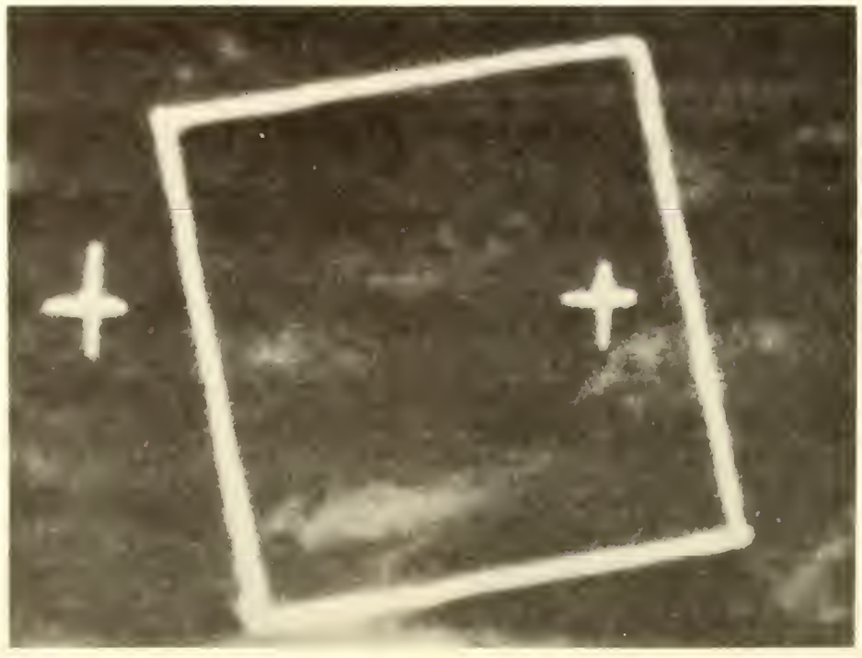

ATS III satellite photograph, June 24, 1969, 1610 GMT.
Displacement 110 km, 020°.

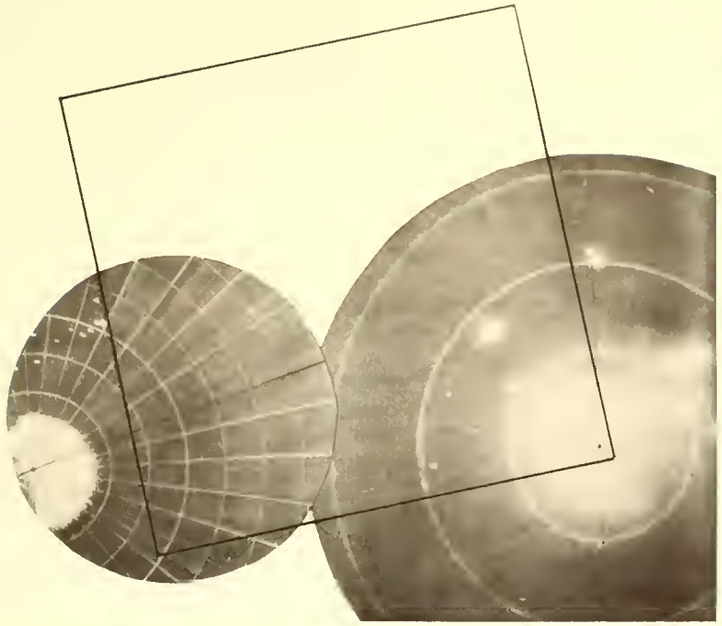

Surface radar composite, June 24, 1969, 2158 GMT.

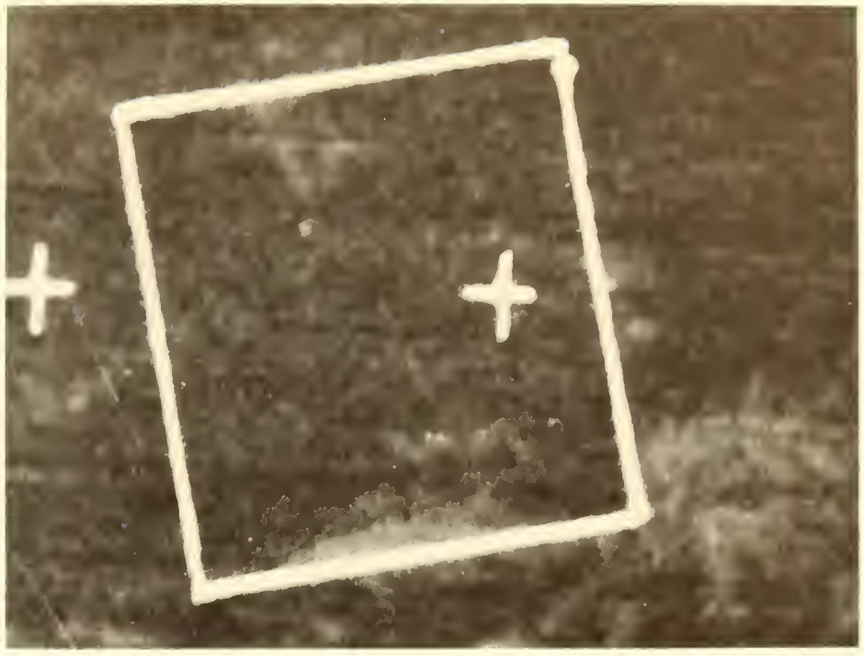

ATS III satellite photograph, June 24, 1969, 2043 GMT.
Displacement 30 km, 170°.

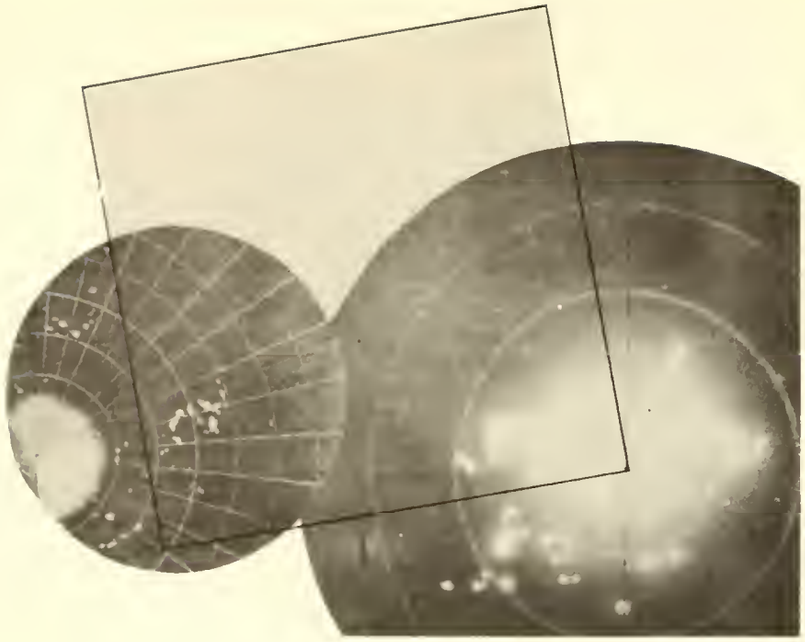

Surface radar composite, June 25, 1969, 0356 GMT.

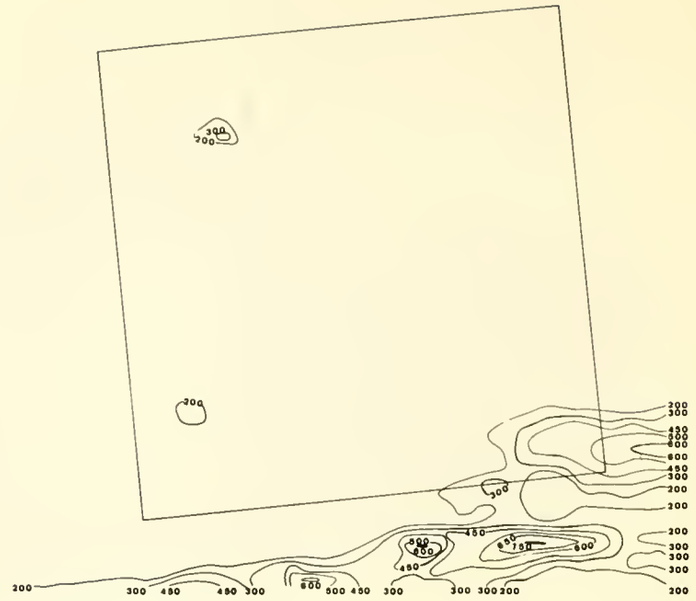

Nimbus 3 HRIR cloud top contour map, June 25, 1969, 0348 GMT.

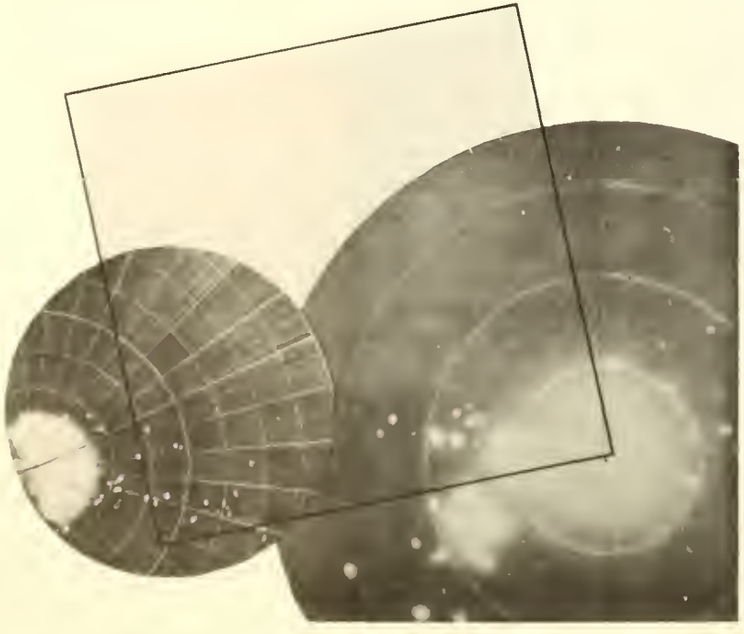

Surface radar composite, June 25, 1969, 0951 GMT.

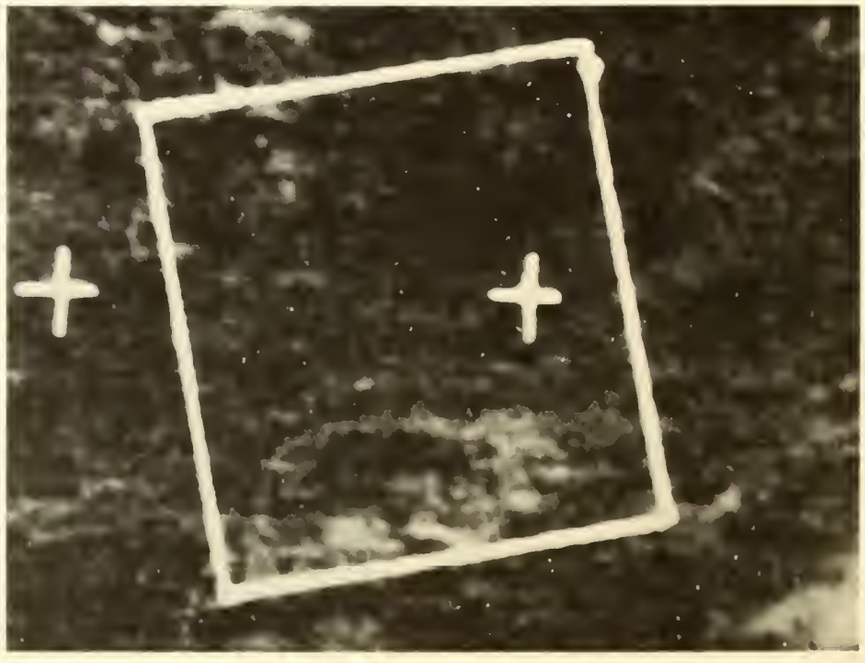

ATS III satellite photograph, June 25, 1969, 1109 GMT.
No displacement.

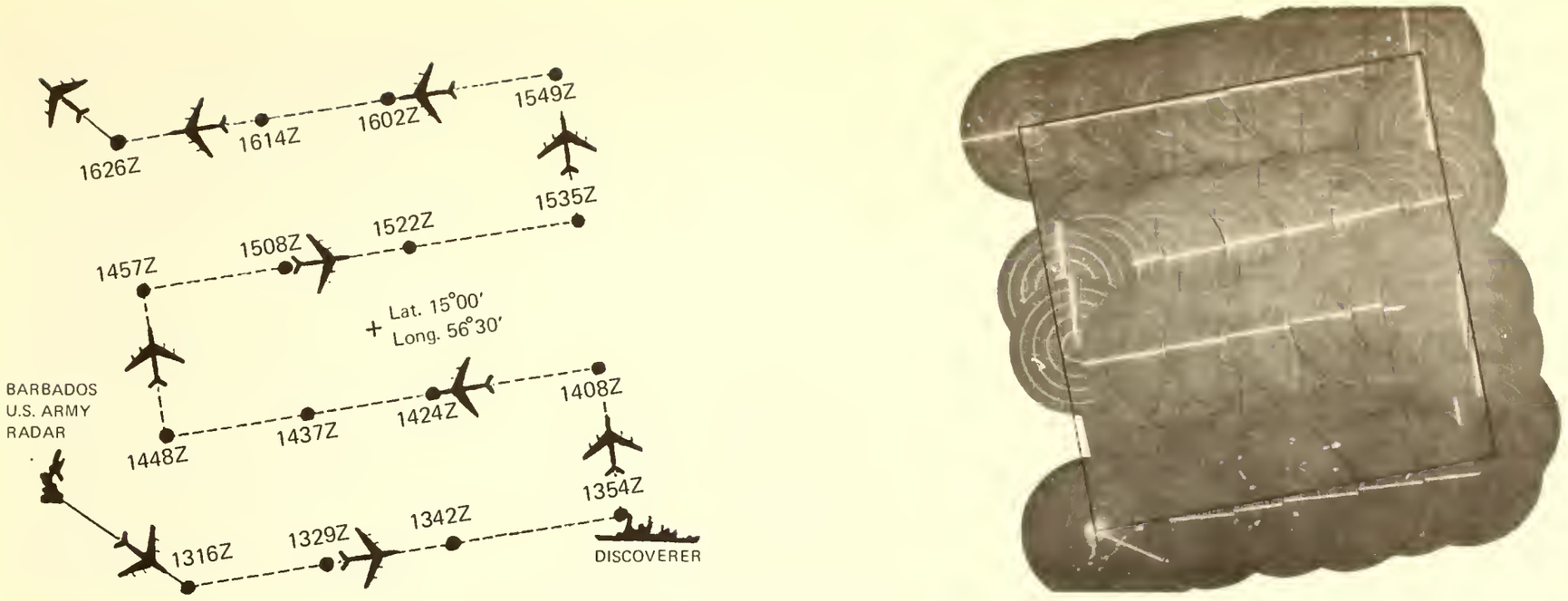

Aircraft flight track and radar mosaic, June 25, 1969, 1316-1626 GMT.

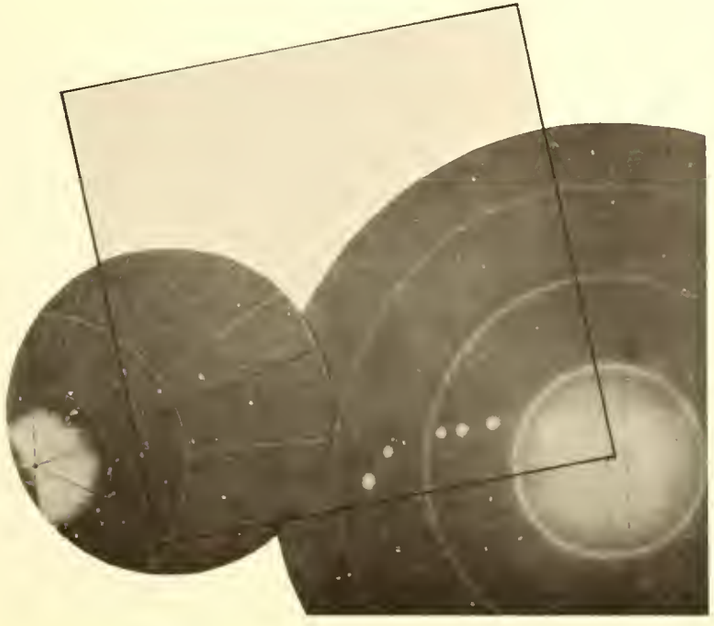

Surface radar composite, June 25, 1969, 1547 GMT.

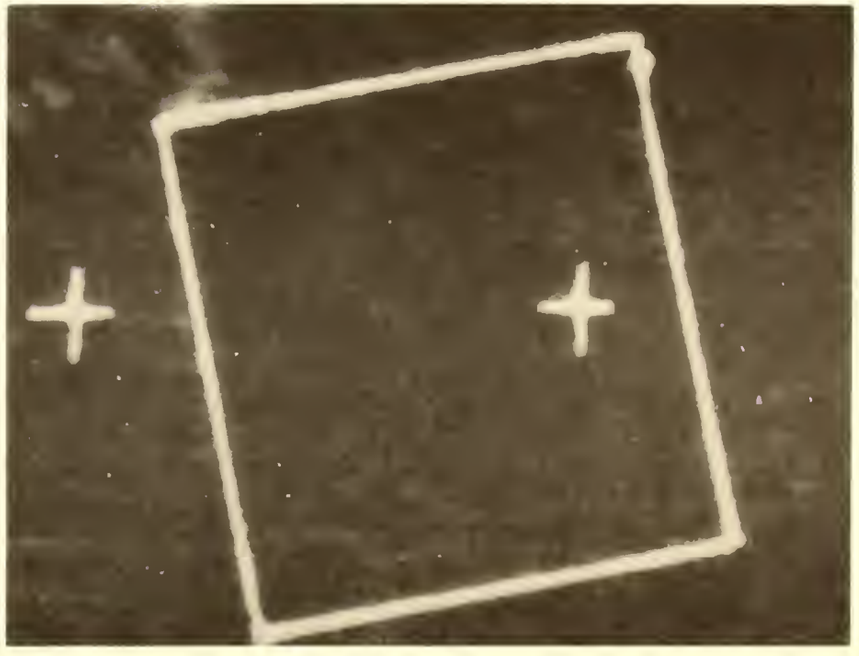

ATS III satellite photograph, June 25, 1969, 1608 GMT.
Displacement 45 km, 220°.

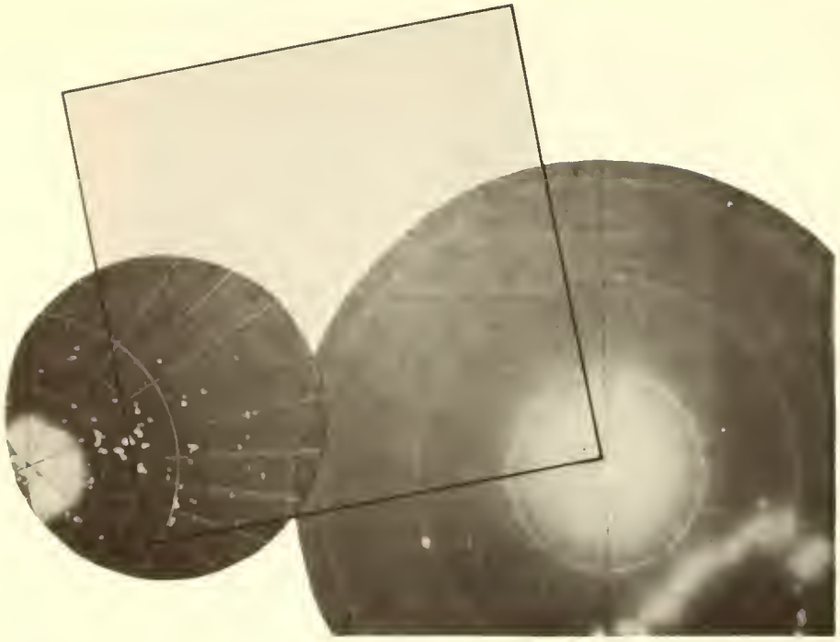

Surface radar composite, June 25, 1969, 2020 GMT.

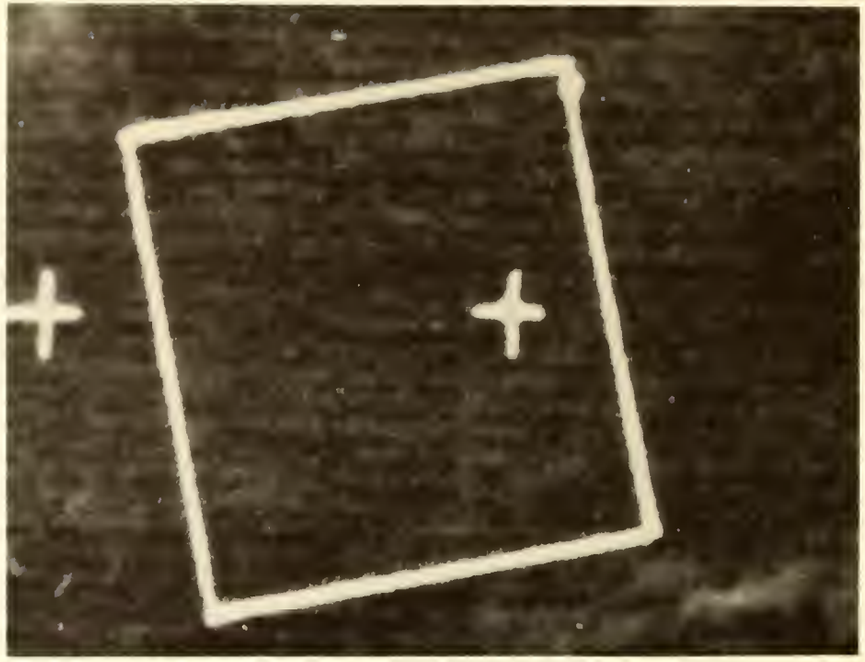

ATS III satellite photograph, June 25, 1969 2035 GMT.
Displacement 110 km, 250°.

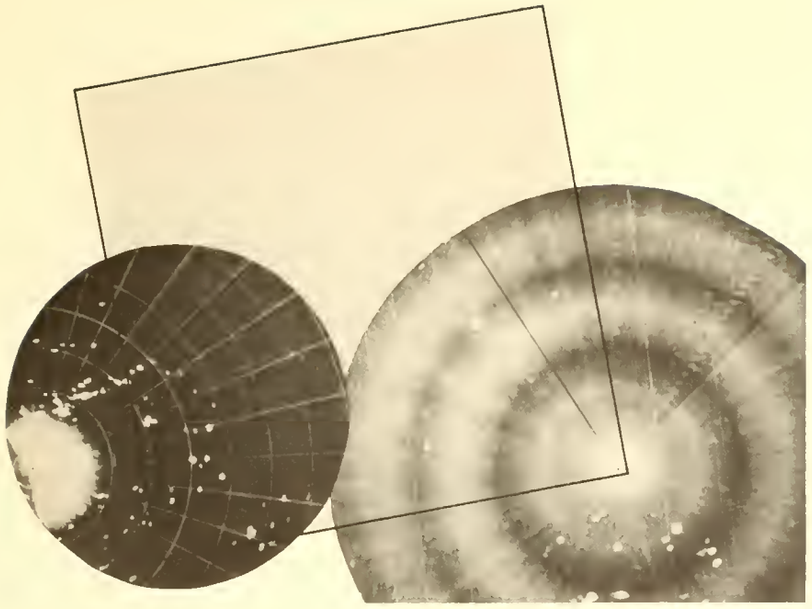

Surface radar composite, June 26, 1969, 0251 GMT.

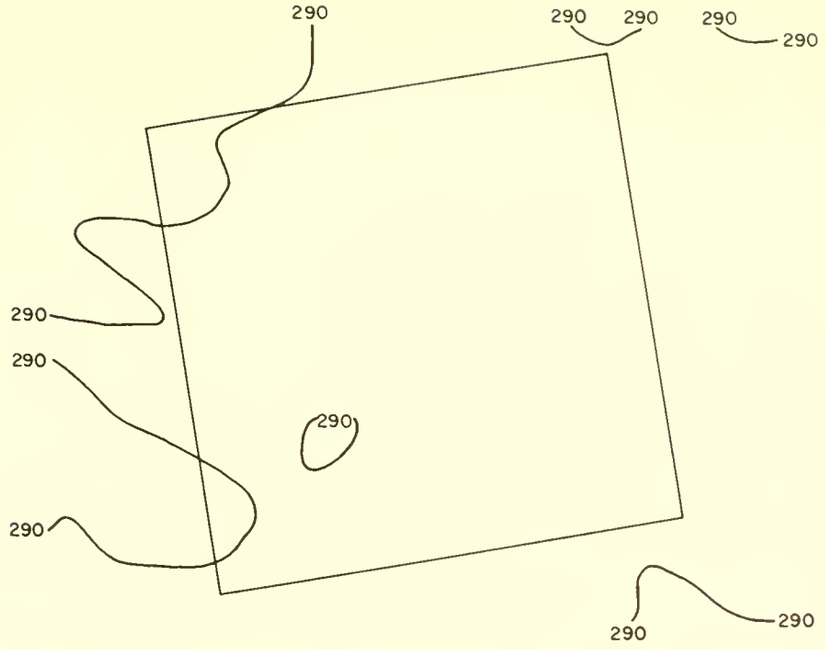

Nimbus 3 MRIR cloud top contour map, June 26, 1969, 0305 GMT.

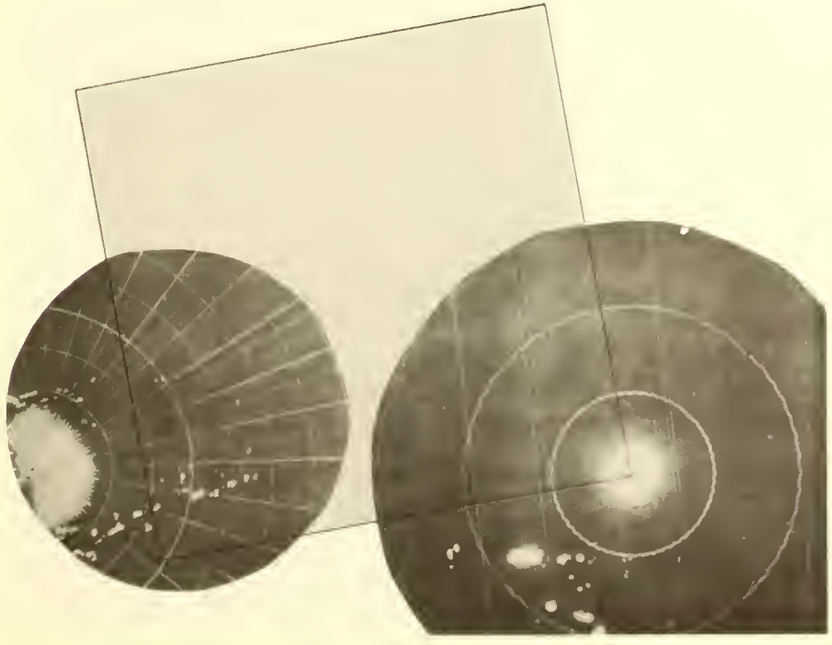

Surface radar composite, June 26, 1969, 1014 GMT.

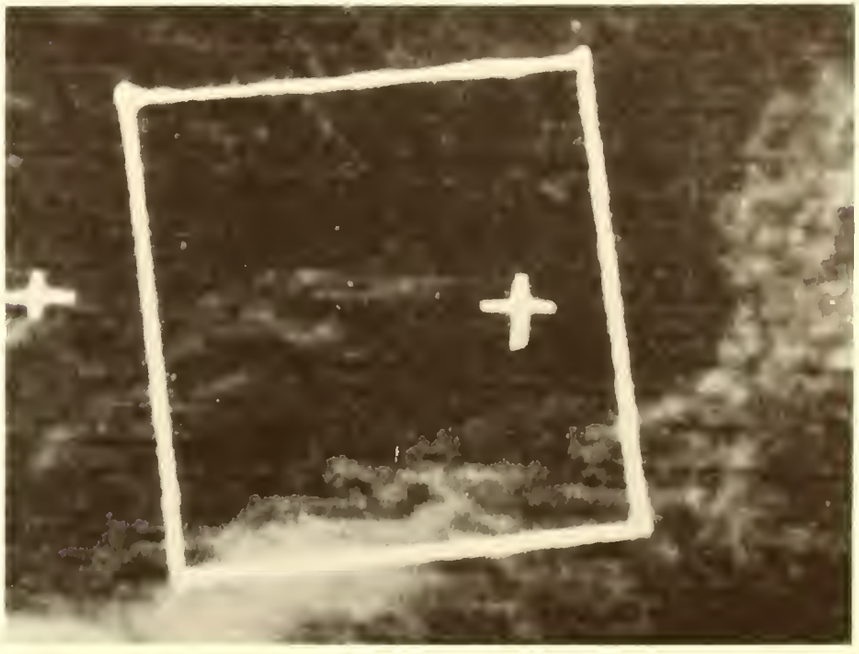

ATS III satellite photograph, June 26, 1969, 1117 GMT.
Displacement 110 km, 220°.

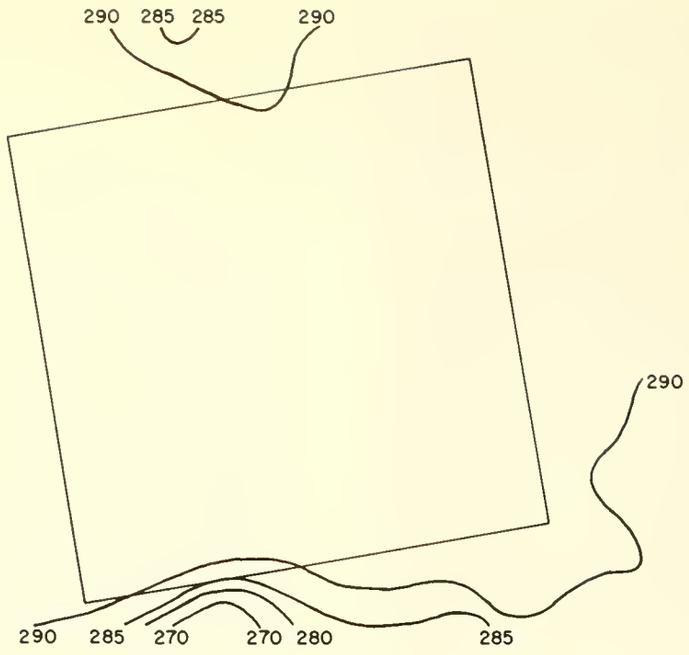

Nimbus 3 MRIR cloud top contour map, June 26, 1969, 1452 GMT.

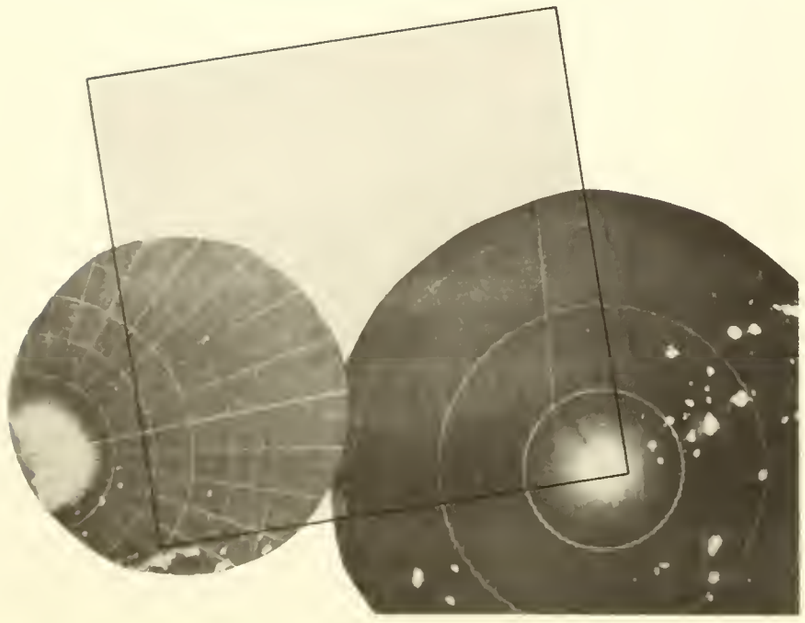

Surface radar composite, June 26, 1969, 1616 GMT.

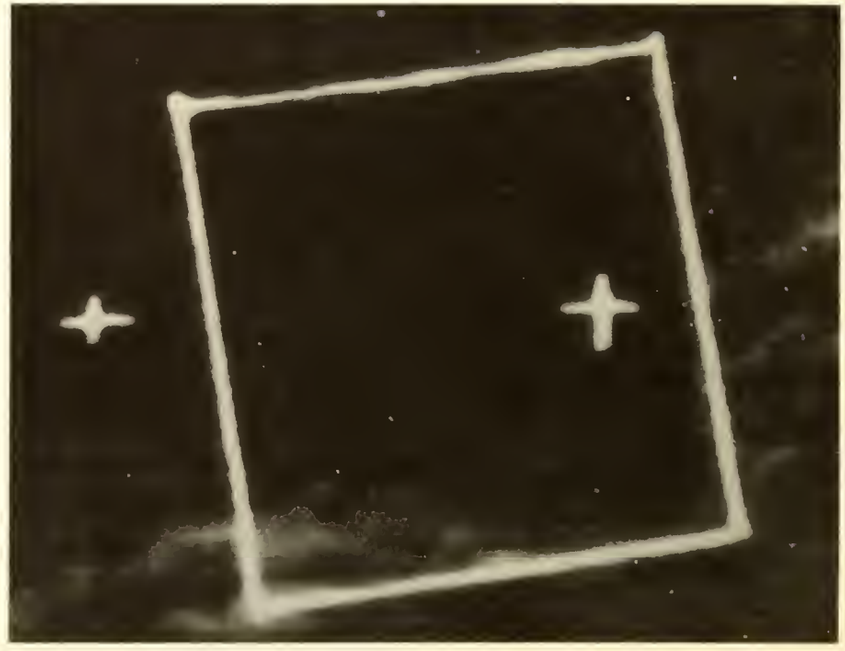

ATS III satellite photograph, June 26, 1969, 1615 GMT.
Displacement 65 km, 320°.

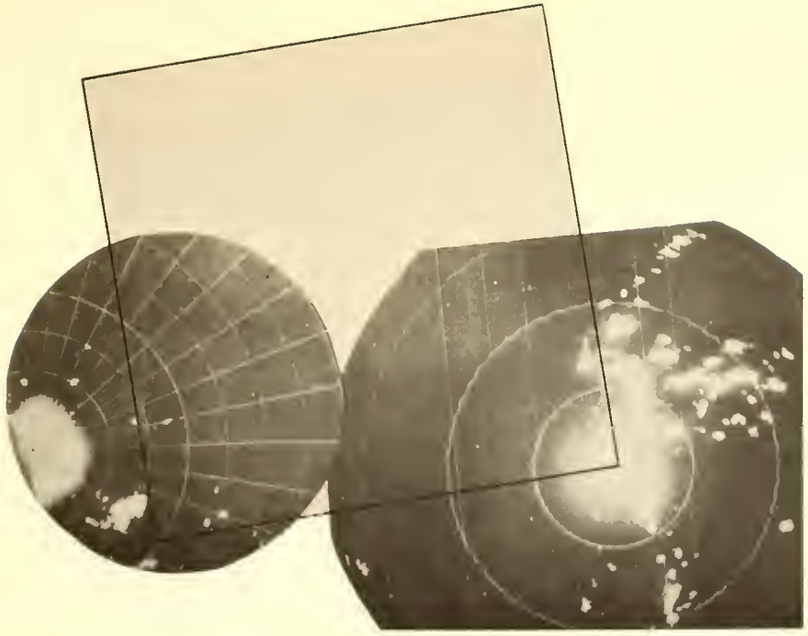

Surface radar composite, June 26, 1969, 2014 GMT.

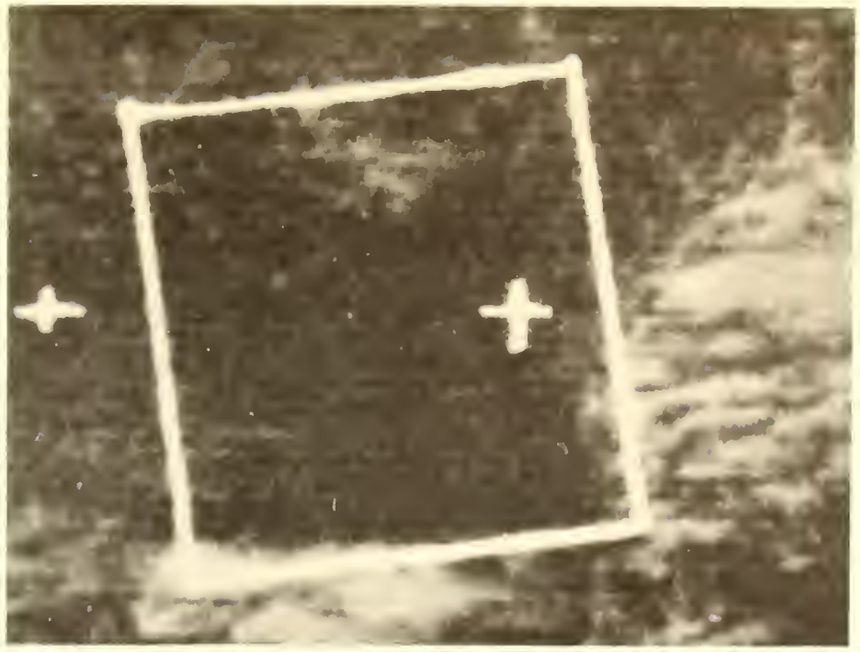

ATS III satellite photograph, June 26, 1969, 2035 GMT.
Displacement 75 km, 170°.

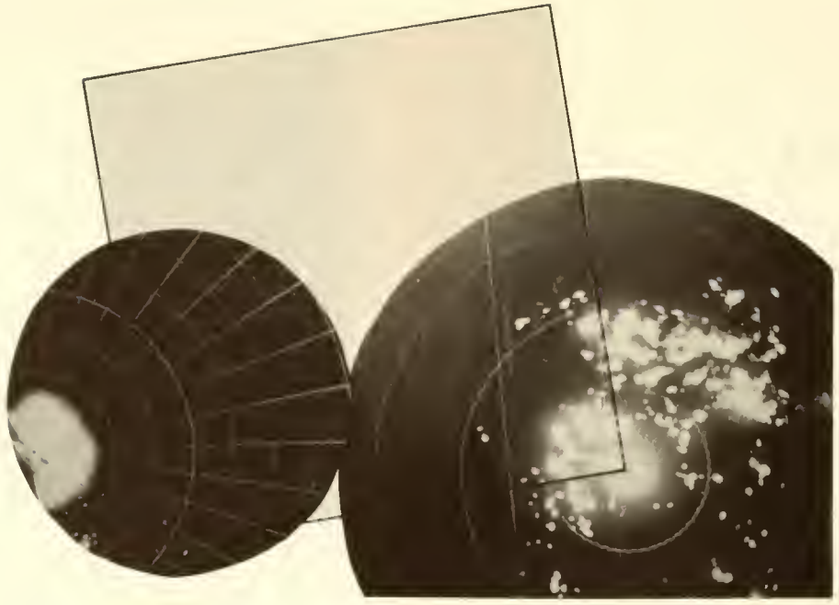

Surface radar composite, June 27, 1969, 0435 GMT.

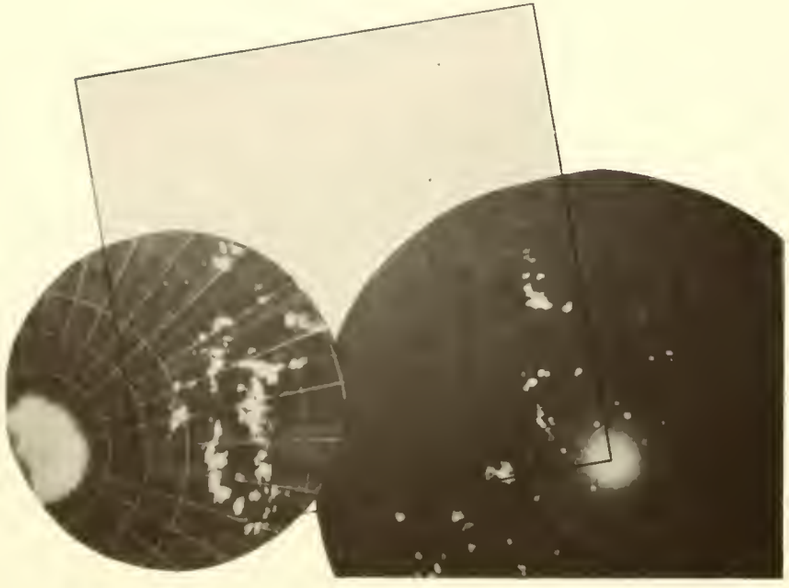

Surface radar composite, June 27, 1969, 1252 GMT.

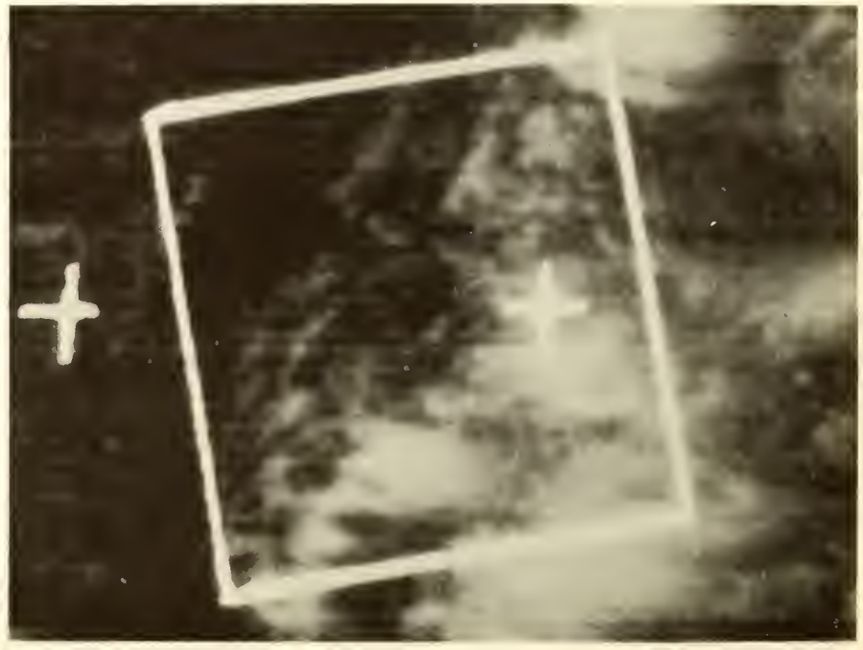

ATS III satellite photograph, June 27, 1969, 1254 GMT.
Displacement 90 km, 185°.

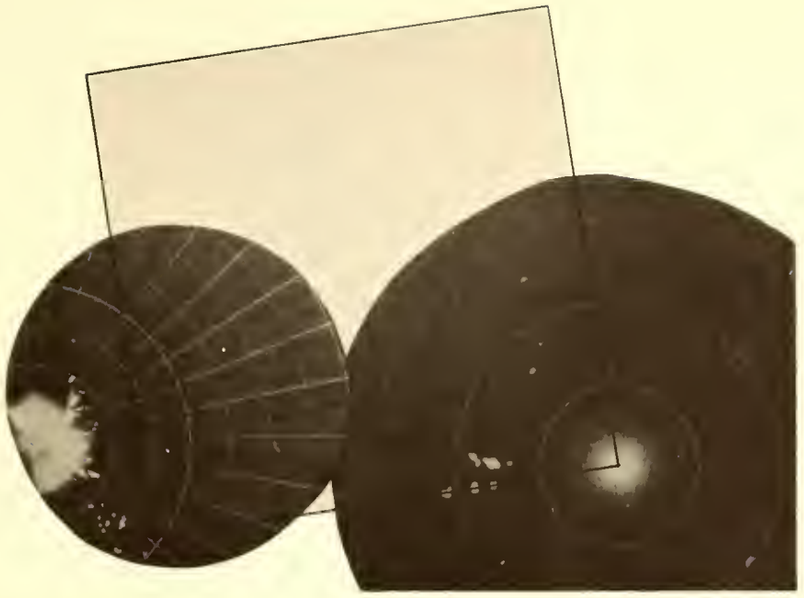

Surface radar composite, June 27, 1969, 1605 GMT.

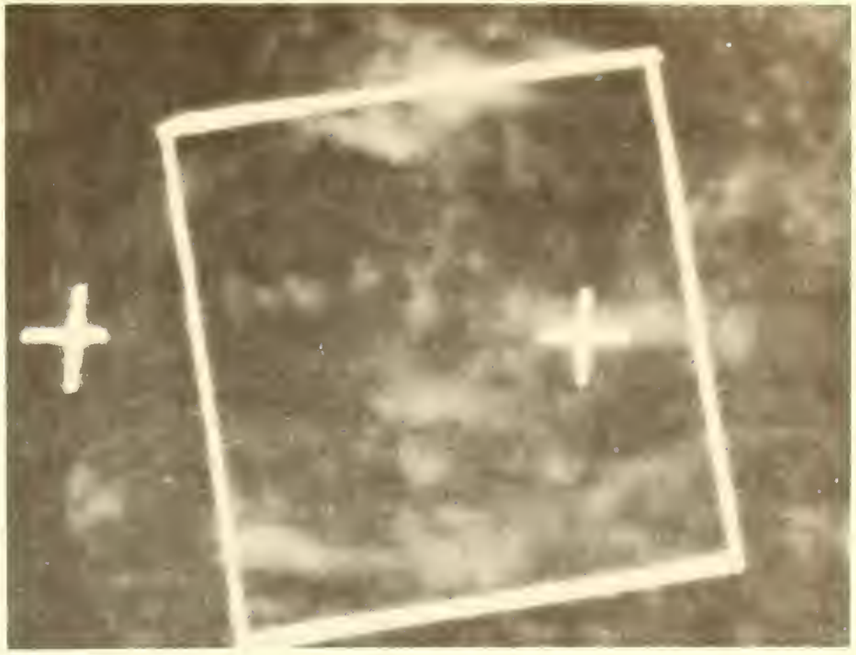

ATS III satellite photograph, June 27, 1969, 1605 GMT.
Displacement 90 km, 270°.

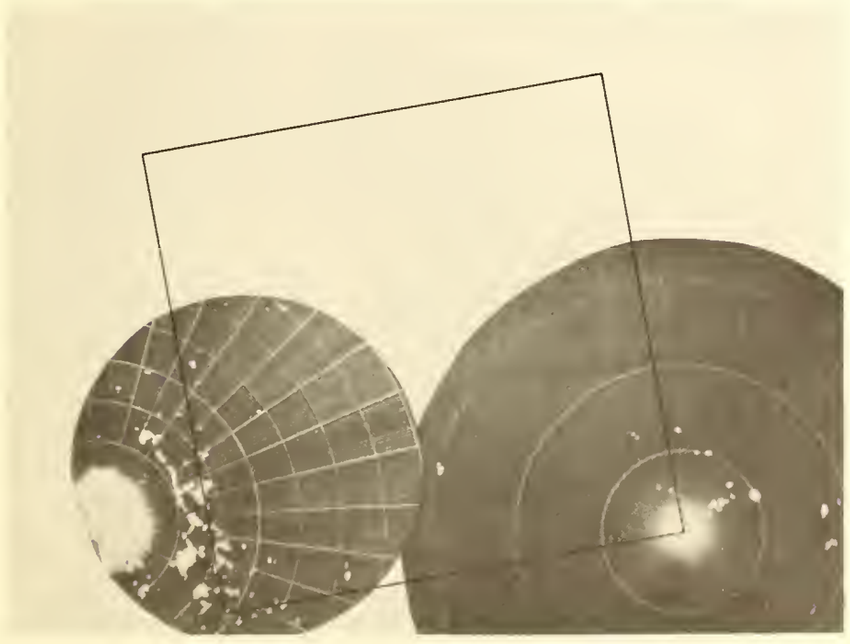

Surface radar composite, June 27, 1969, 2029 GMT.

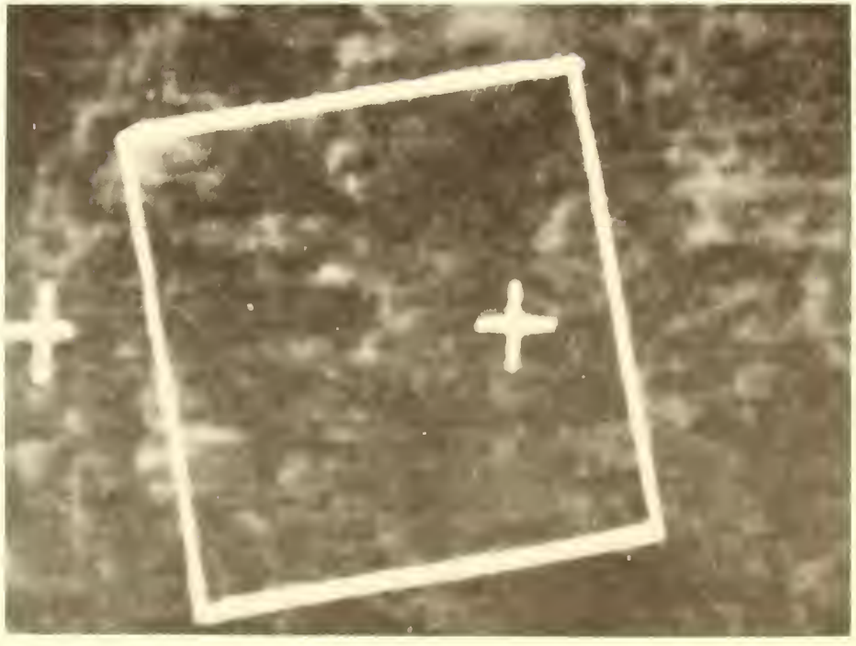

ATS III satellite photograph, June 27, 1969, 2028 GMT.
No displacement.

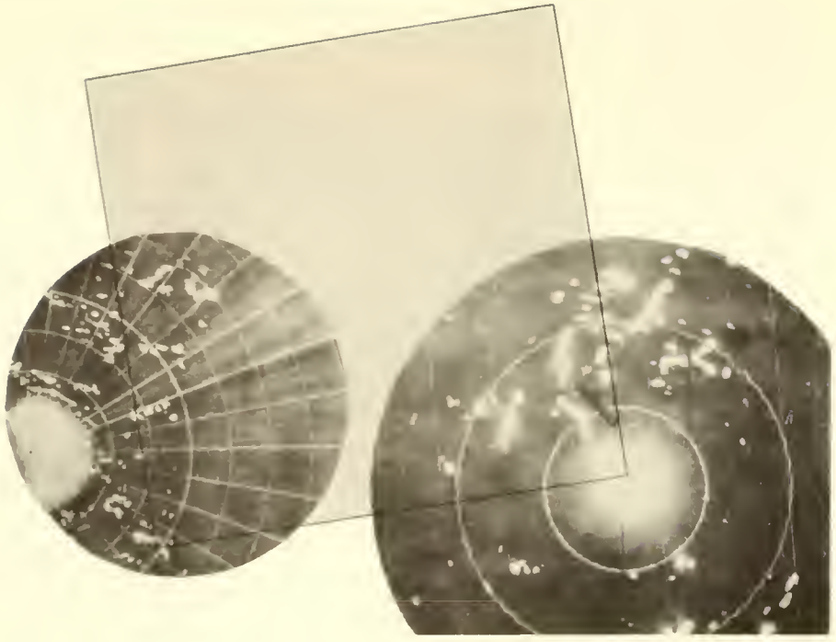

Surface radar composite, June 28, 1969, 0329 GMT.

Nimbus 3 HRIR cloud top contour map, June 28, 1969, 0324 GMT.

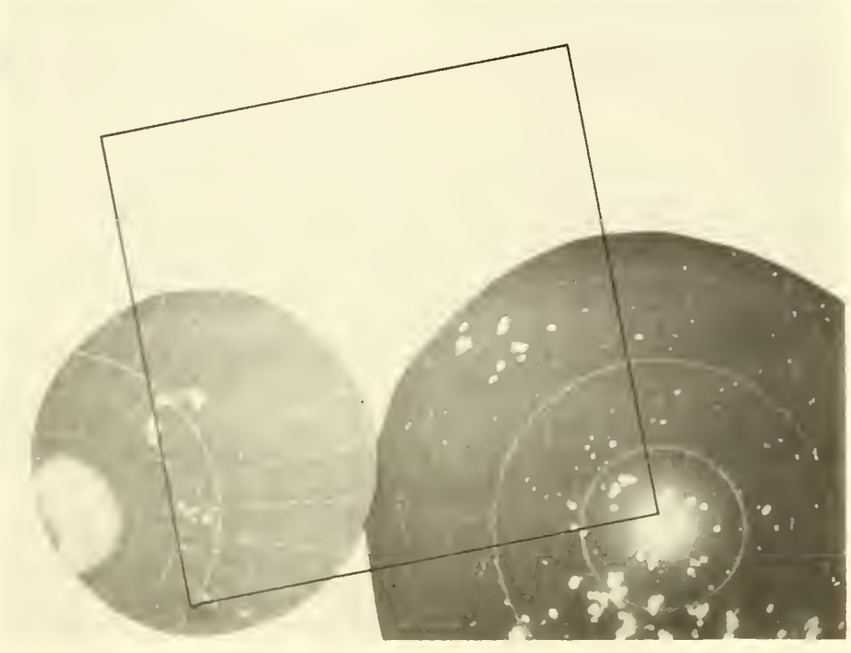

Surface radar composite, June 28, 1969, 1057 GMT.

ATS III satellite photograph, June 28, 1969, 1108 GMT,
Displacement 100 km, 060°.

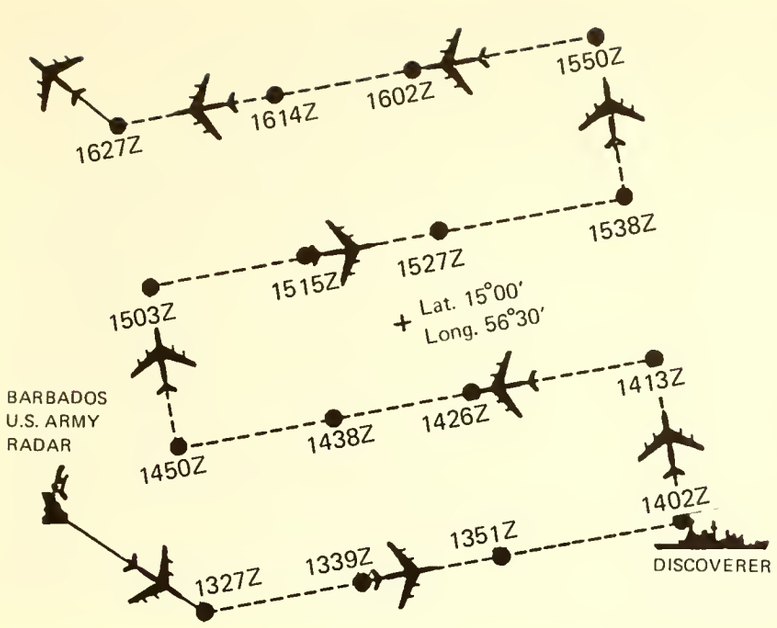

Aircraft flight track and radar mosaic, June 28, 1969, 1327-1627 GMT.

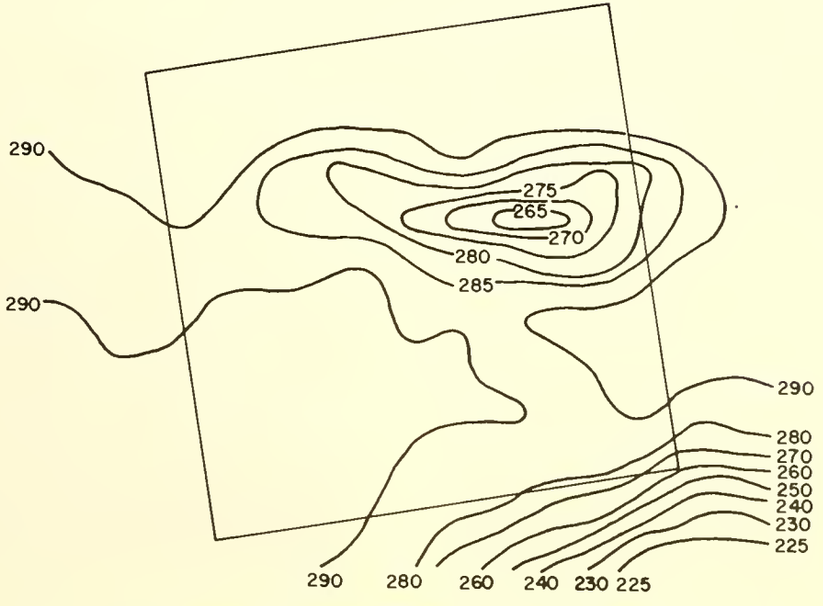

Nimbus 3 MRIR cloud top contour map, June 28, 1969, 1512 GMT.

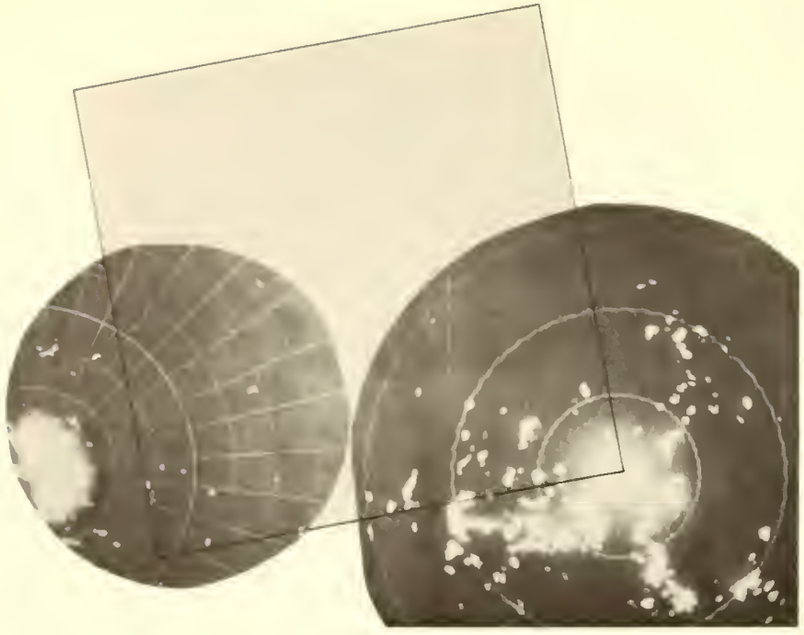

Surface radar composite, June 28, 1969, 1602 GMT.

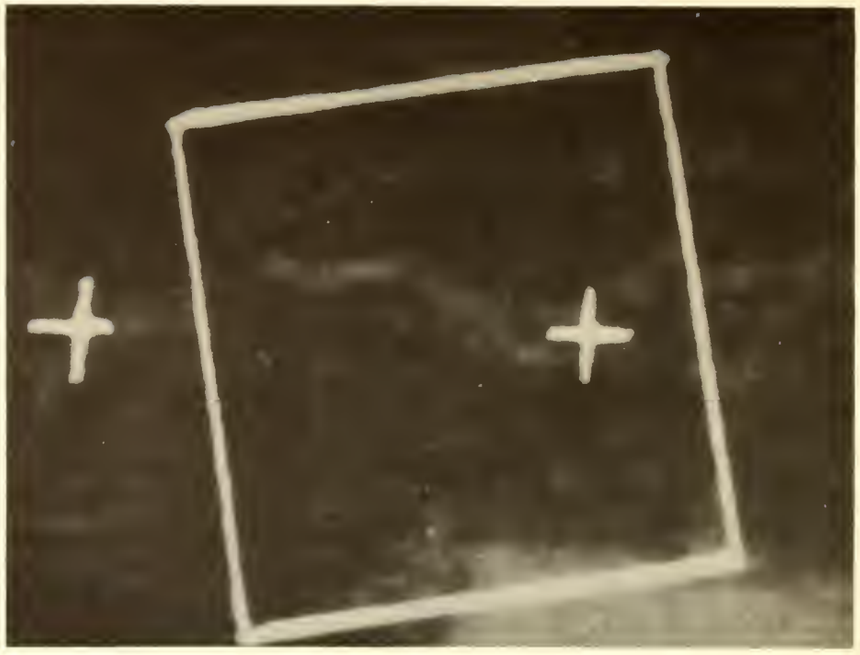

ATS III satellite photograph, June 28, 1969, 1614 GMT.
Displacement 45 km, 240°.

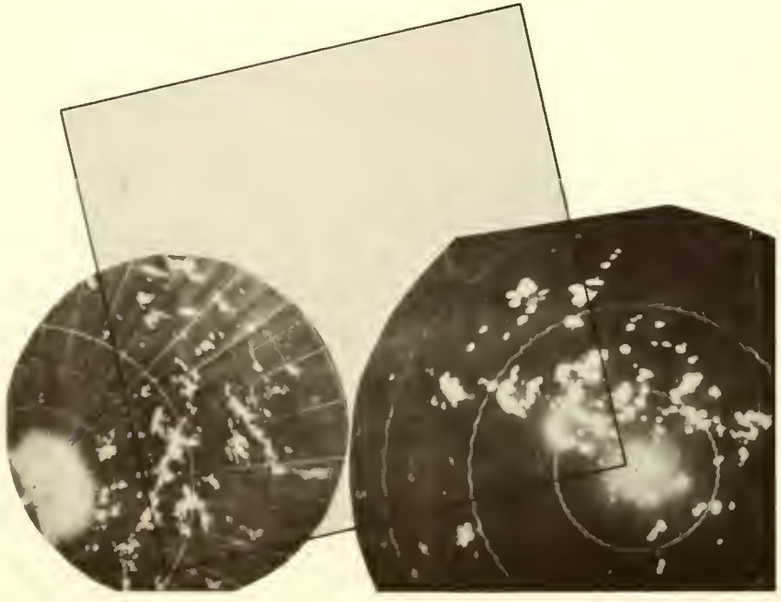

Surface radar composite, June 28, 1969, 2021 GMT.

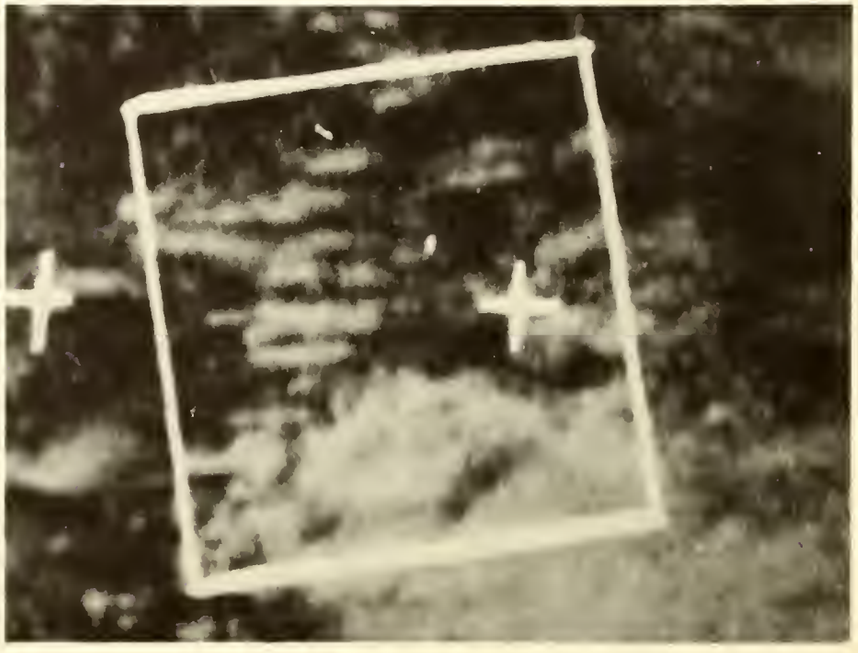

ATS III satellite photograph, June 28, 1969, 2020 GMT.
Displacement 55 km, 150°.

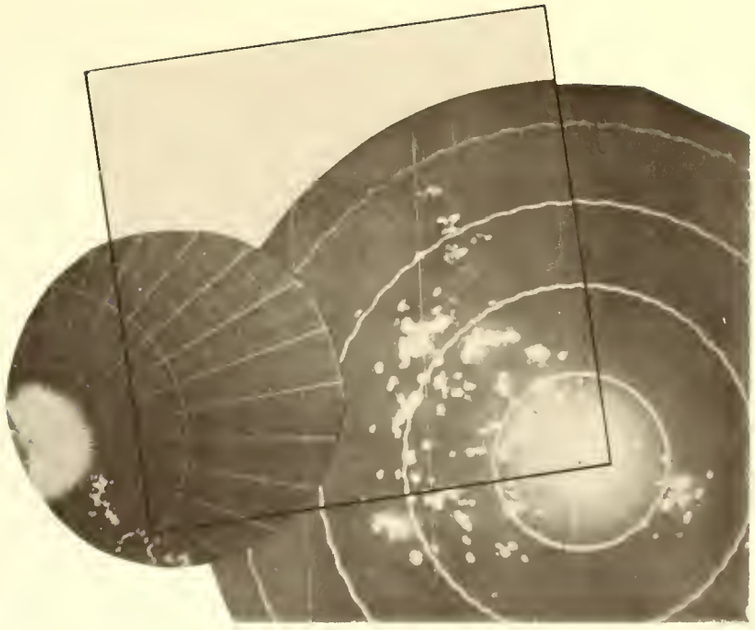

Surface radar composite, June 29, 1969, 0232 GMT.

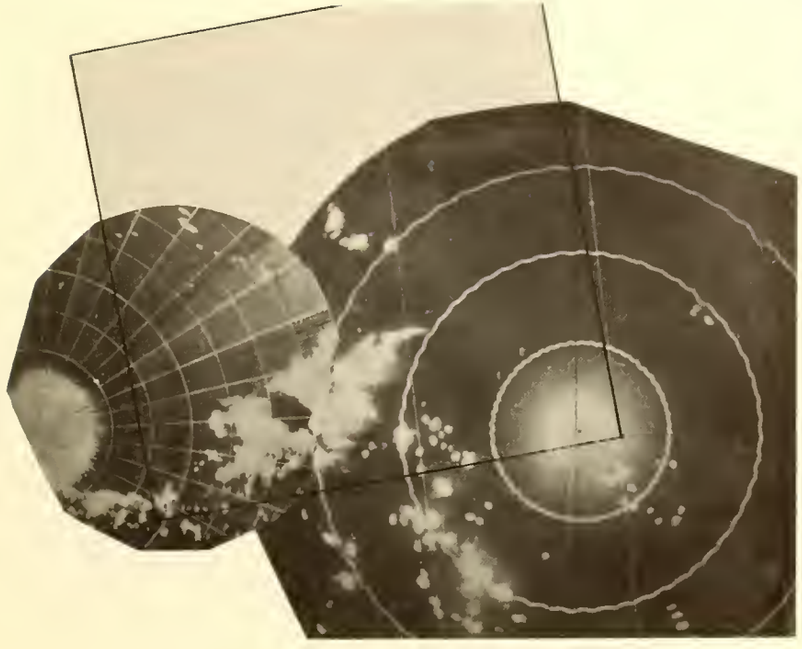

Surface radar composite, June 29, 1969, 1122 GMT.

ATS III satellite photograph, June 29, 1969, 1119 GMT.
No displacement .

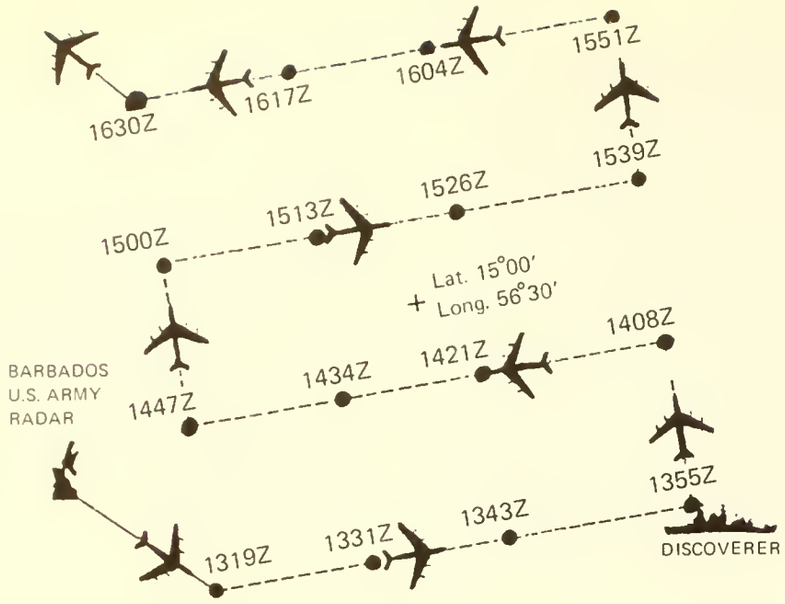

Aircraft flight track and radar mosaic, June 29, 1969, 1319-1630 GMT.

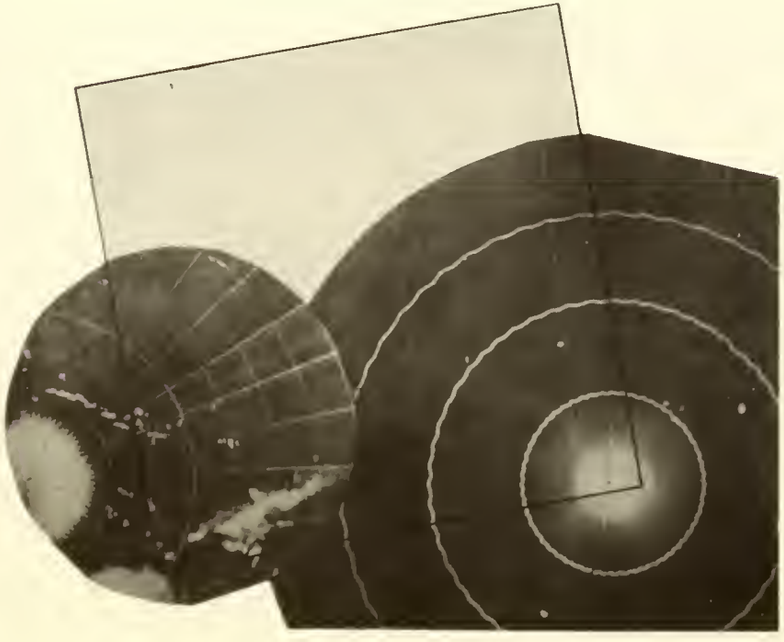

Surface radar composite, June 29, 1969, 1558 GMT.

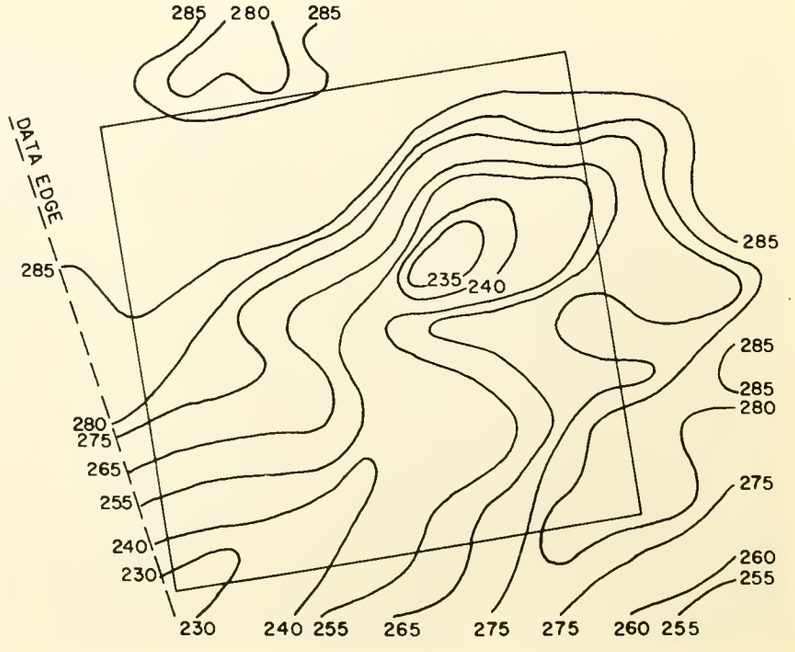

Nimbus 3 MRIR cloud top contour map, June 29, 1969, 1430 GMT.

ATS III satellite photograph, June 29, 1969, 1706 GMT.
Displacement 45 km, 020°.

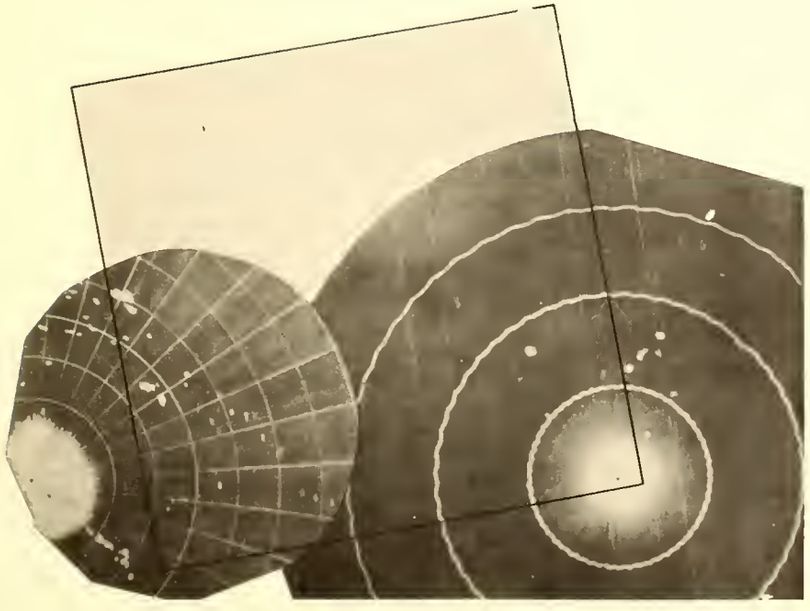

Surface radar composite, June 29, 1969, 2038 GMT.

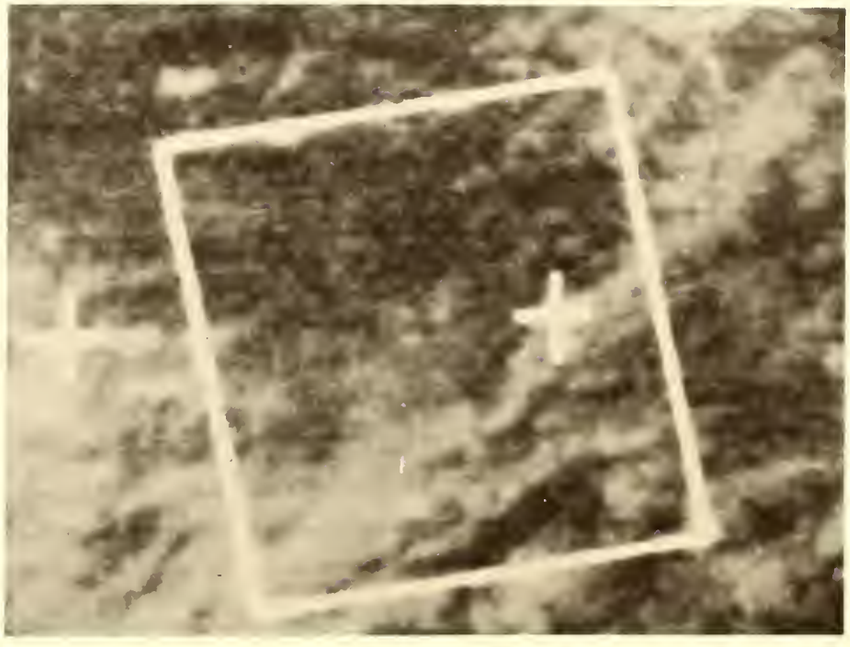

ATS III satellite photograph, June 29, 1969, 2040 GMT.
Displacement 75 km, 195°.

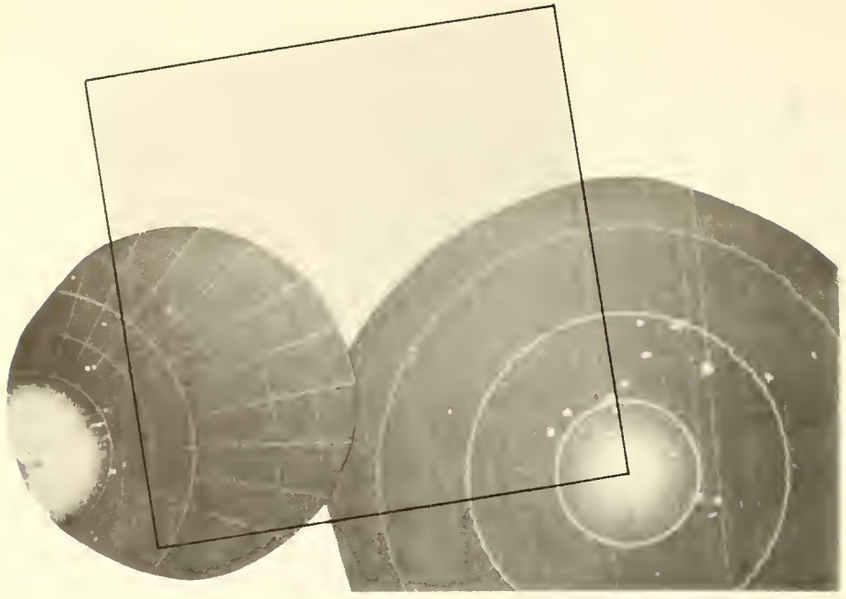

Surface radar composite, June 30, 1969, 0349 GMT.

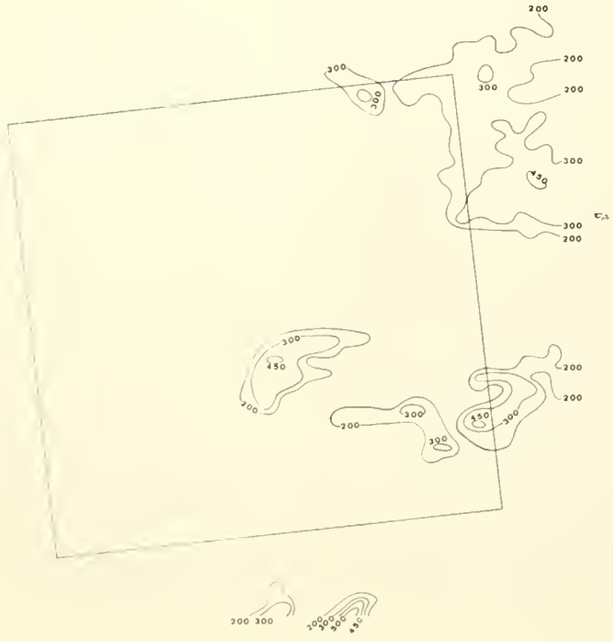

Nimbus 3 HRIR cloud top contour map, June 30, 1969, 0344 GMT.

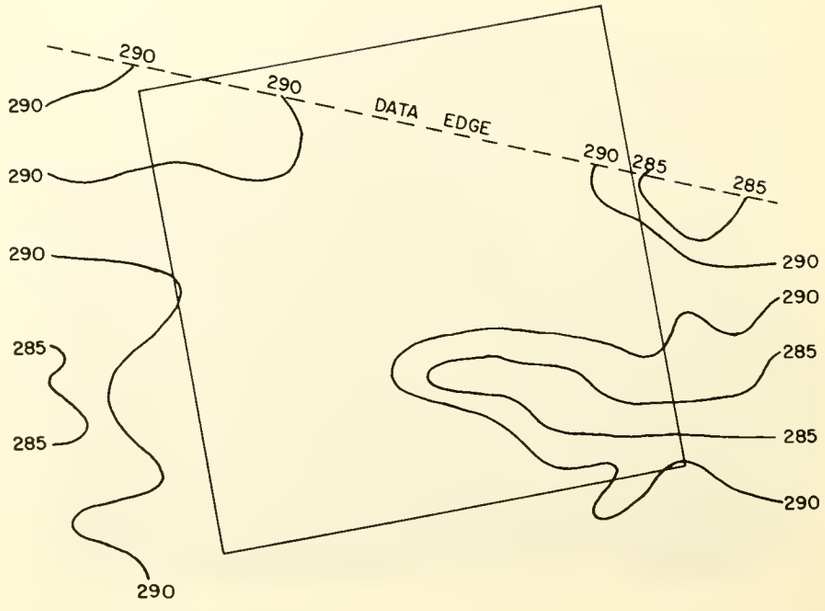

Nimbus 3 MRIR cloud top contour map, June 30, 1969, 0345 GMT.

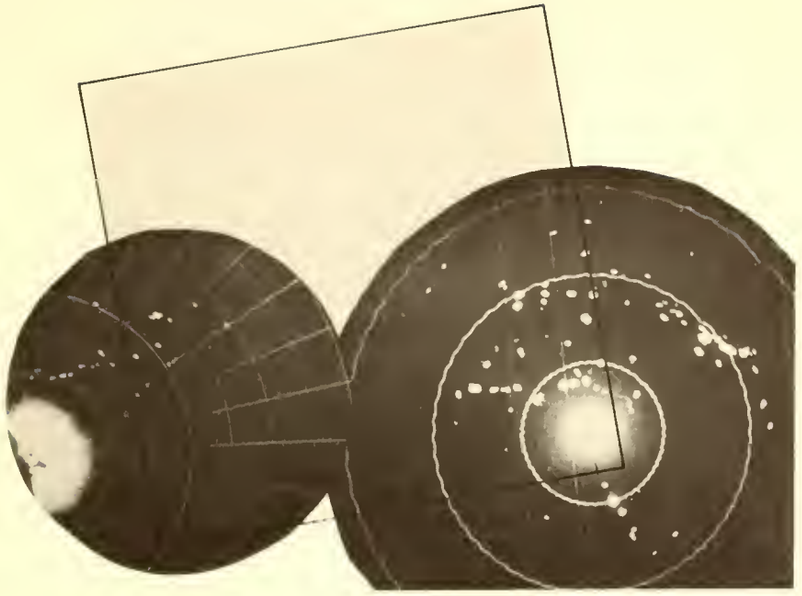

Surface radar composite, June 30, 1969, 1120 GMT.

ATS III satellite photograph, June 30, 1969, 1110 GMT.
Displacement 40 km, 220°.

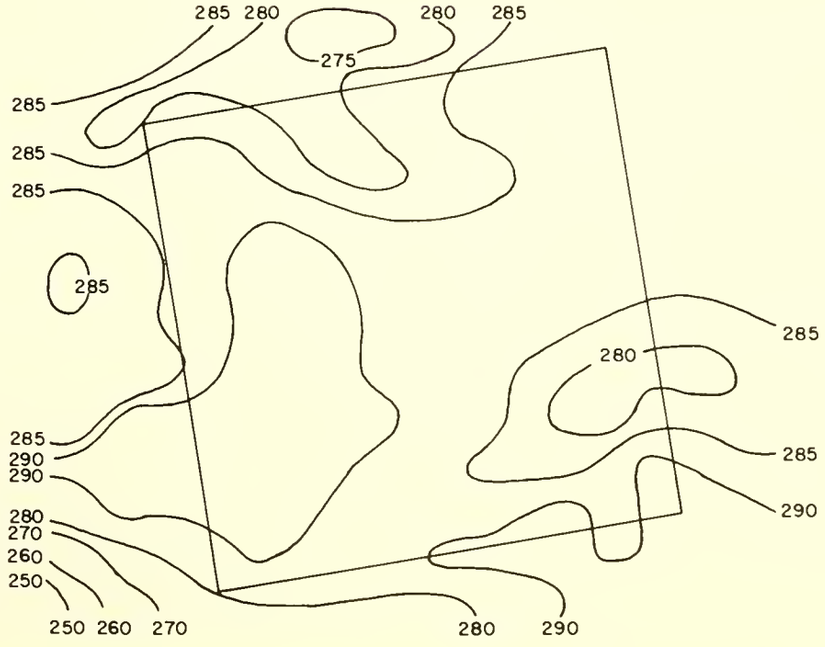

Nimbus 3 MRIR cloud top contour map, June 30, 1969, 1532 GMT.

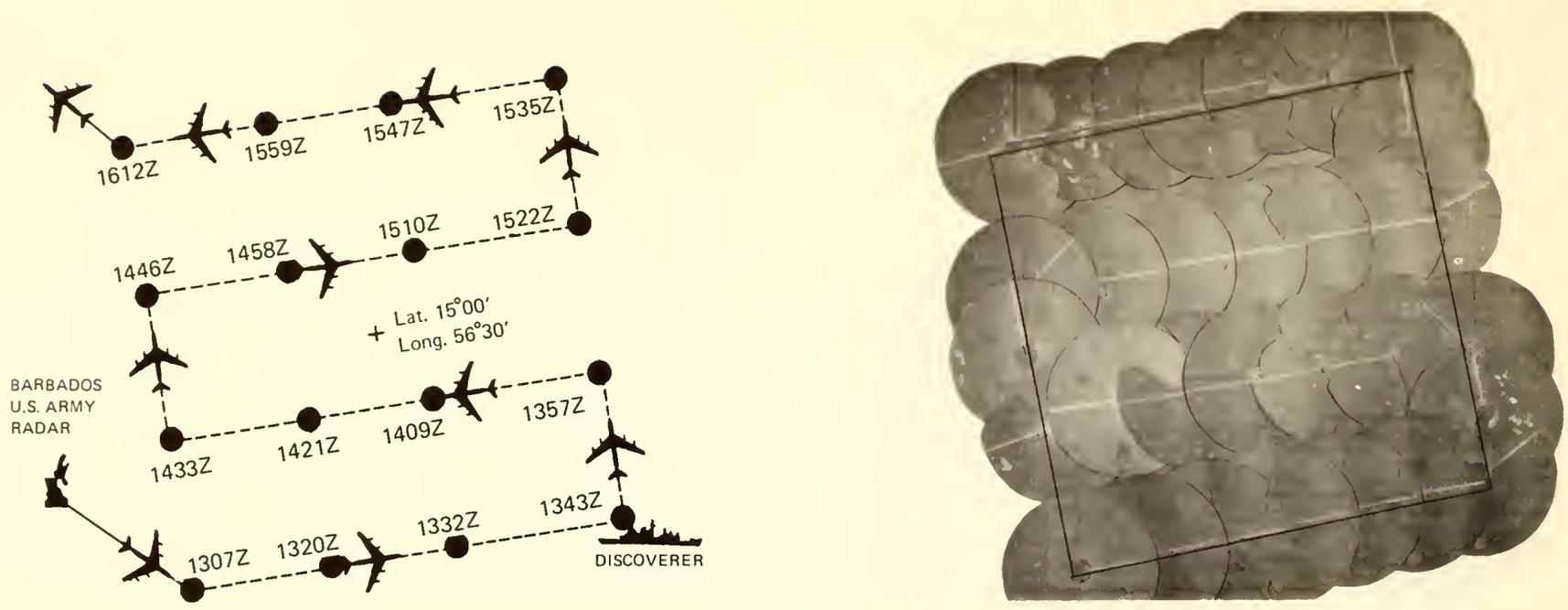

Aircraft flight track and radar mosaic, June 30, 1969, 1307-1612 GMT.

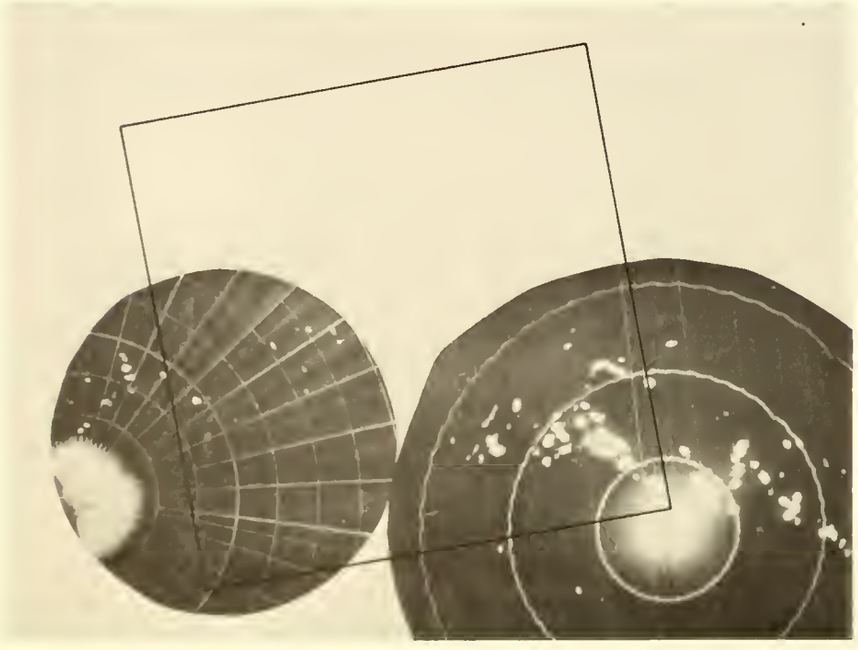

Surface radar composite, June 30, 1969, 1623 GMT.

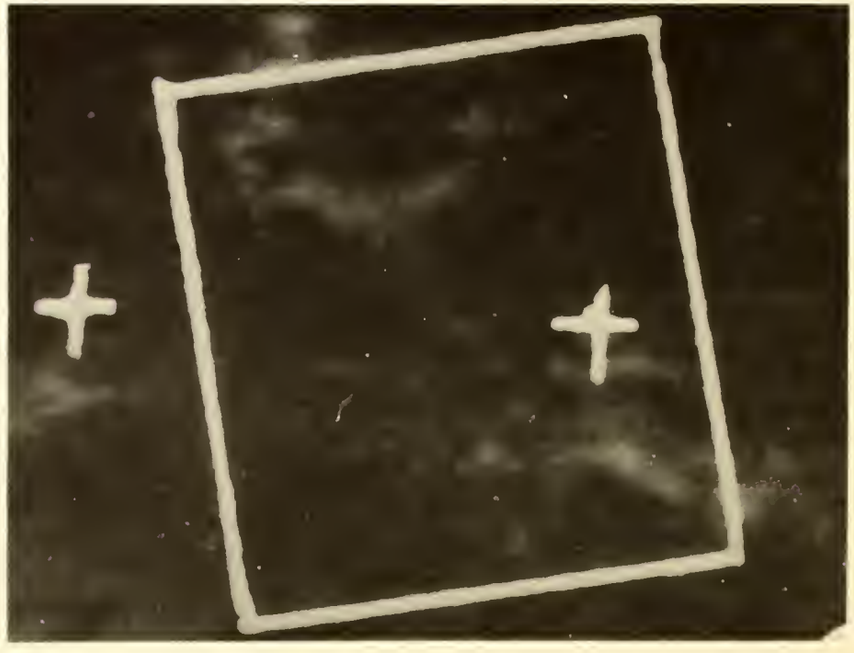

ATS III satellite photograph, June 30, 1969, 1625 GMT.
Displacement 65 km, 230°.

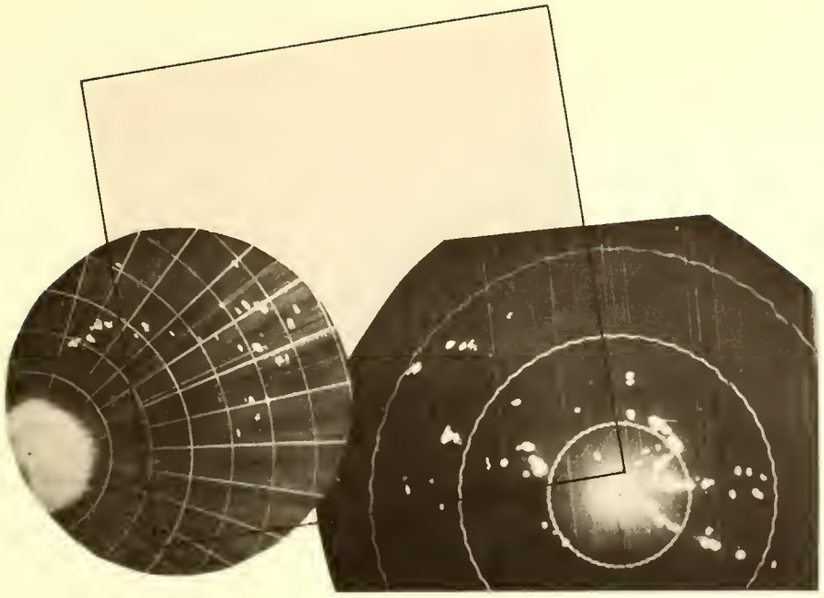

Surface radar composite, June 30, 1969, 2020 GMT.

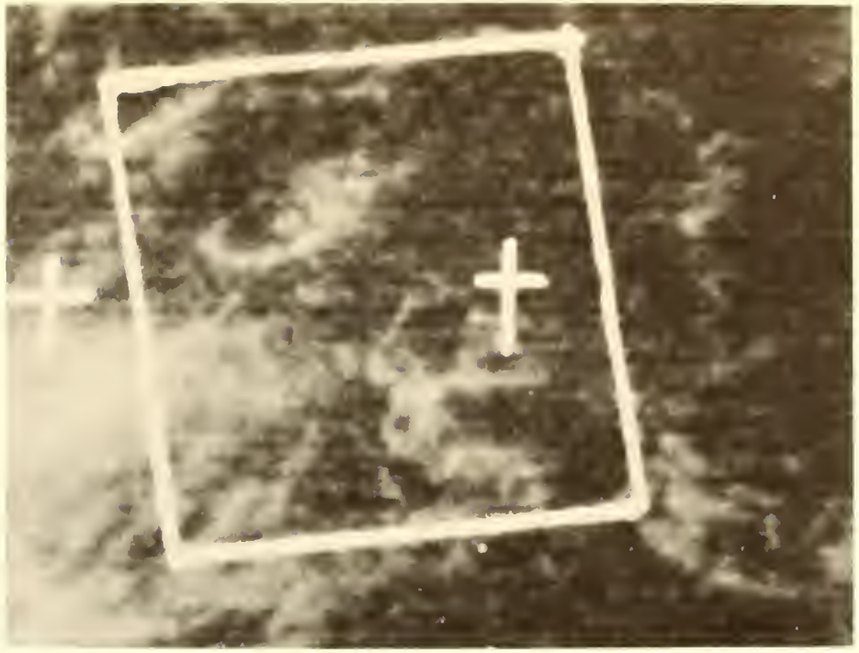

ATS III satellite photograph, June 30, 1969, 2033 GMT.
Displacement 30 km, 150°.

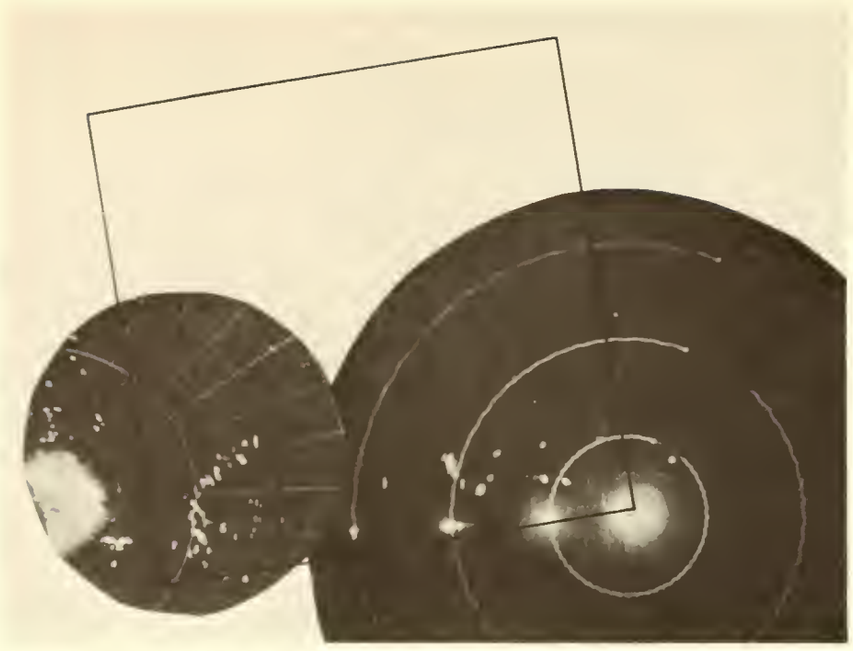

Surface radar composite, July 1, 1969, 0340 GMT.

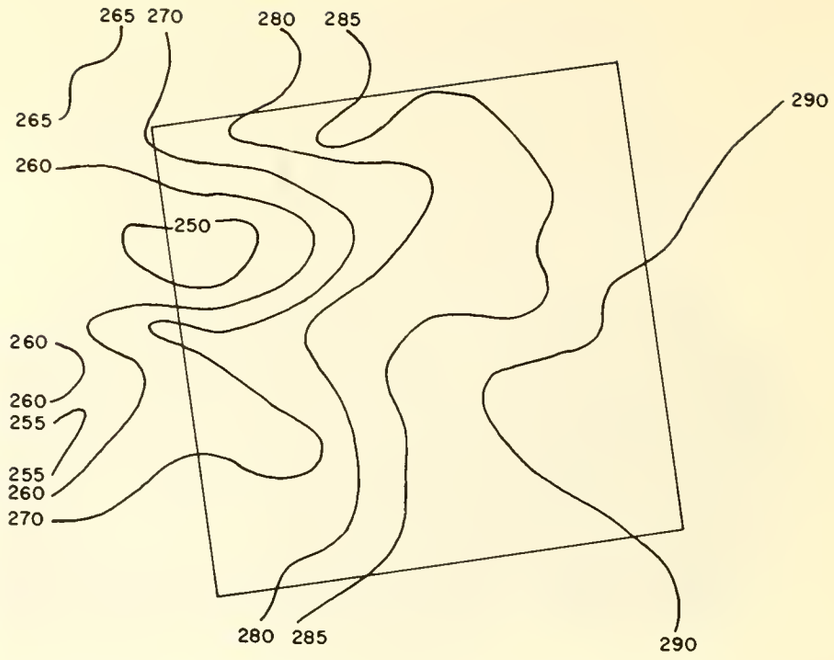

Nimbus 3 MRIR cloud top contour map, July 1, 1969, 0301 GMT.

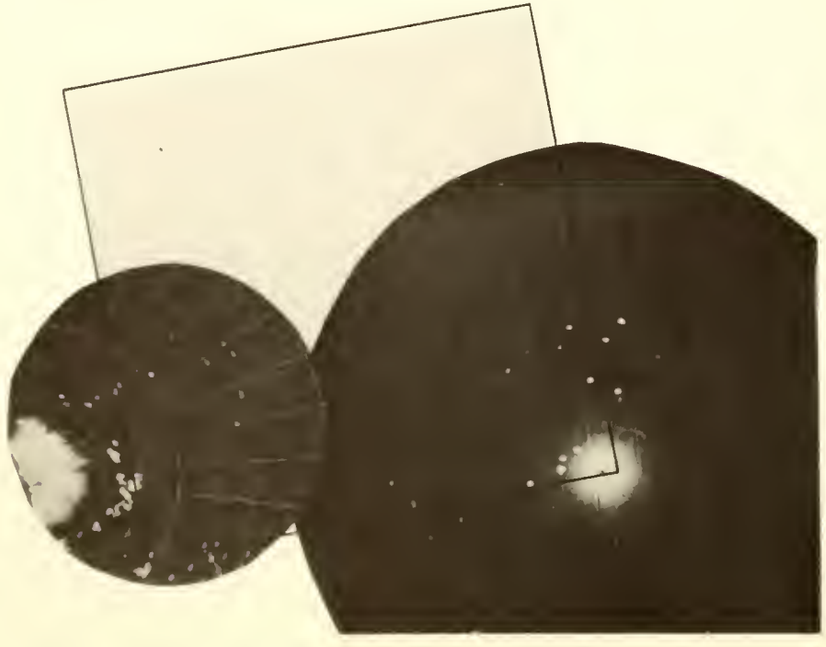

Surface radar composite, July 1, 1969, 1122 GMT.

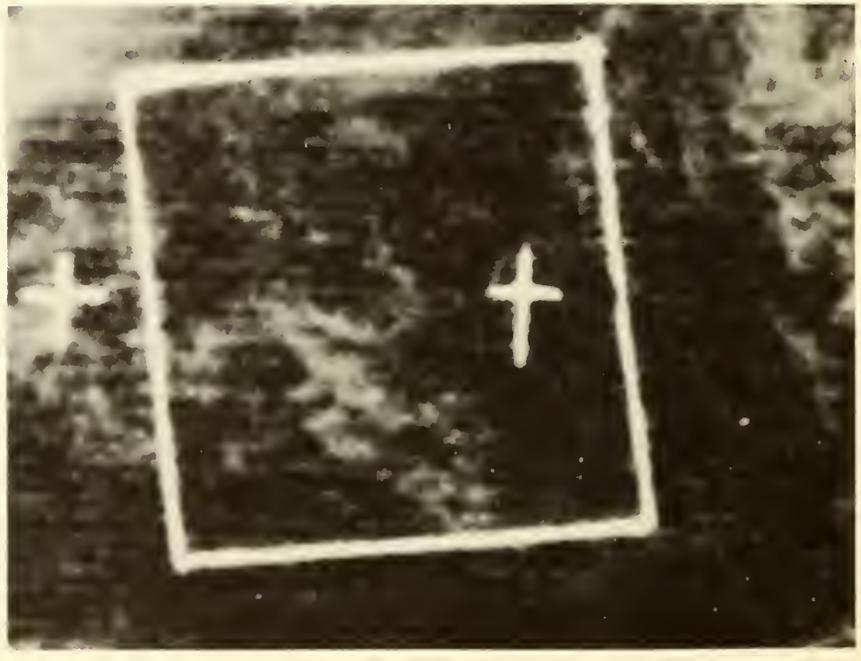

ATS III satellite photograph, July 1, 1969, 1120 GMT.
Displacement 45 km, 070°.

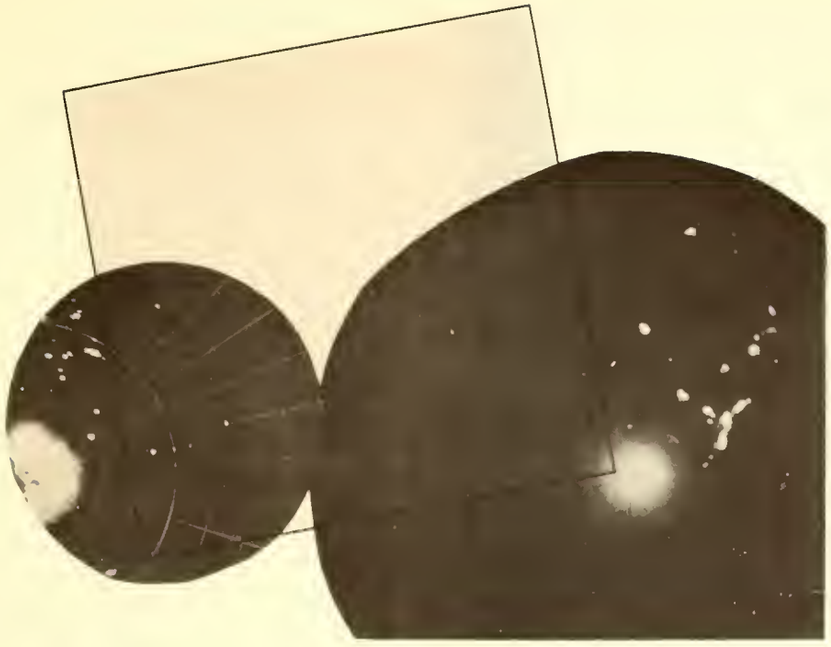

Surface radar composite, July 1, 1969, 1614 GMT.

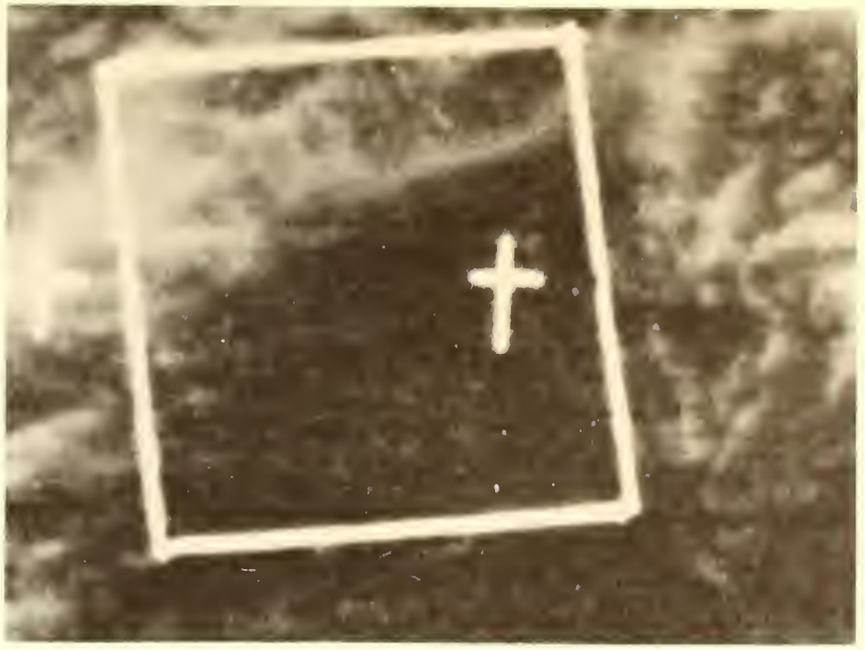

ATS III satellite photograph, July 1, 1969, 1609 GMT.
Displacement 30 km, 140°.

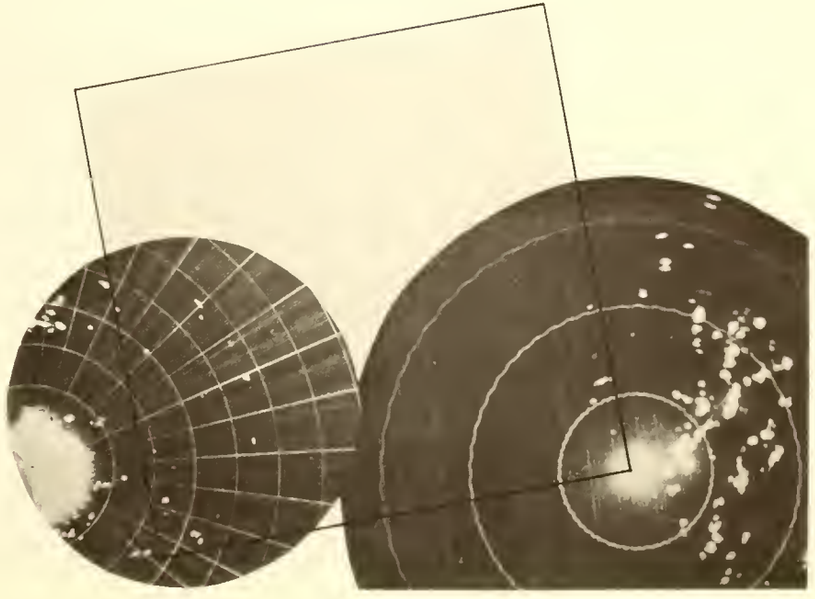

Surface radar composite, July 1, 1969, 2031 GMT.

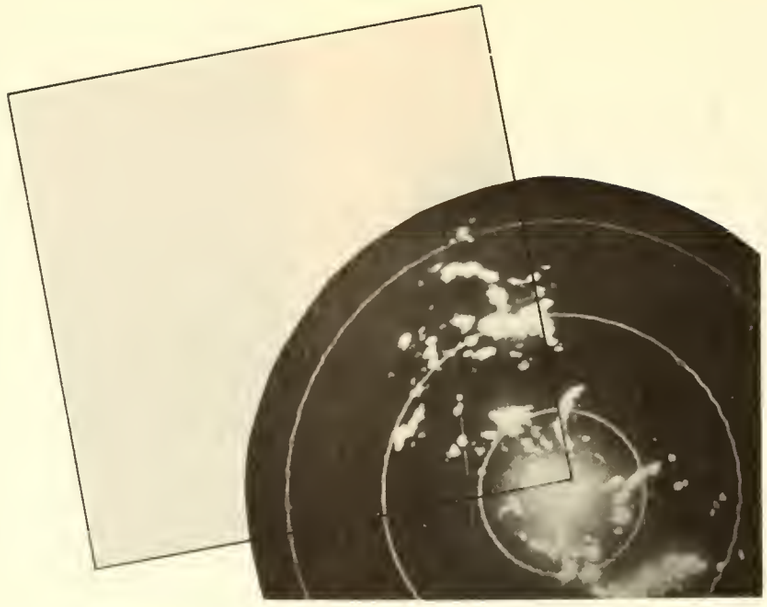

Surface radar composite, July 2, 1969, 0329 GMT.

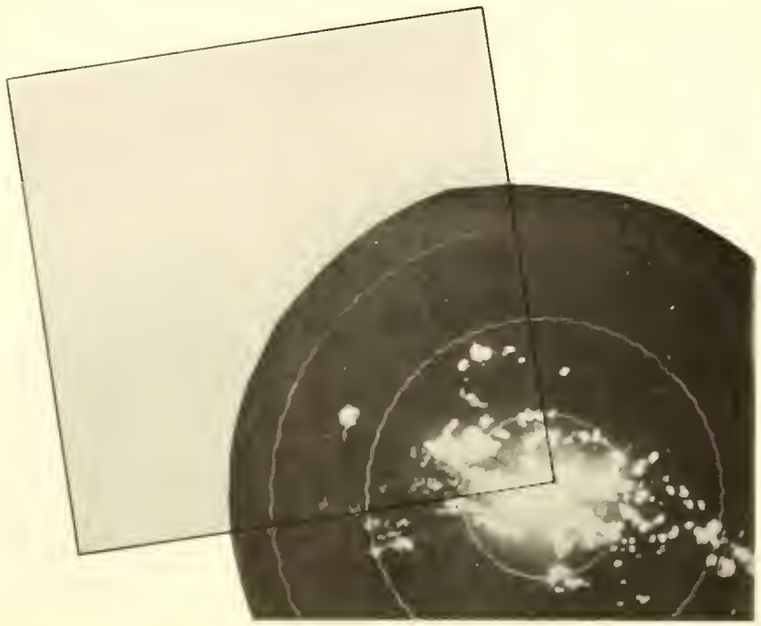

Surface radar composite, July 2, 1969, 1116 GMT.

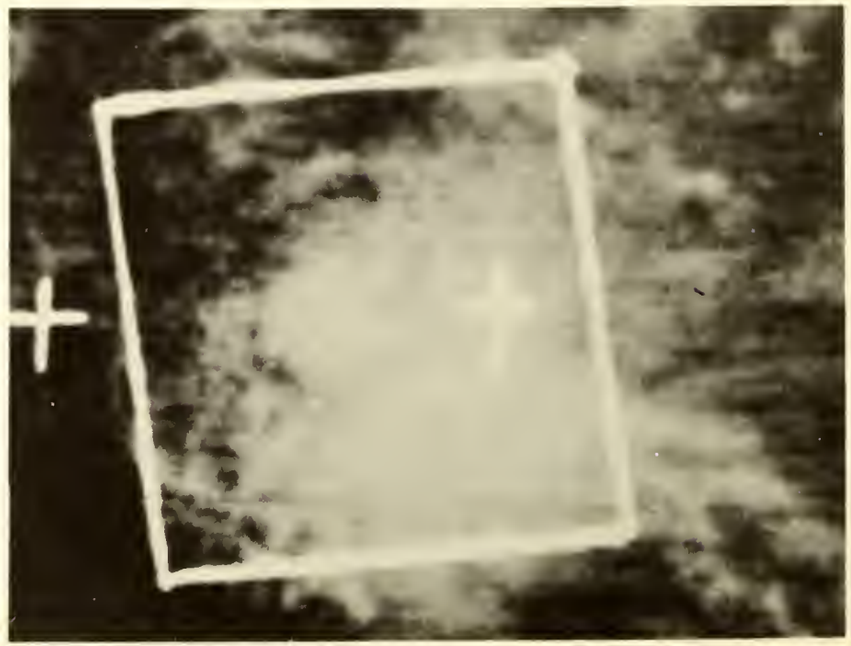

ATS III satellite photograph, July 2, 1969, 1121 GMT.
Displacement 75 km, 270°.

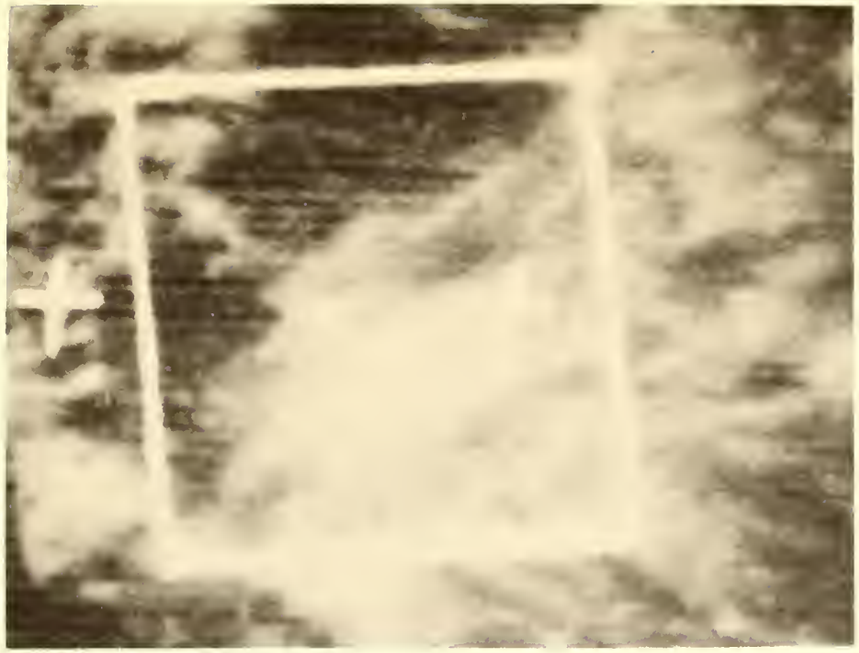

ATS III satellite photograph, July 2, 1969, 1555 GMT.
Displacement 65 km, 265°.

ATS III satellite photograph, July 2, 1969, 2036 GMT. No displacement.

☆ U. S. GOVERNMRNT PRINTING OFFICE : 1975 O - 568-640

BOMEX Period III Radar-Satellite Atlas